Gene 496 (2012) 79–87

Contents lists available at SciVerse ScienceDirect

Gene

journal homepage: www.elsevier.com/locate/gene

Detergent-induced activation of the hepatitis C virus genotype 1b RNA polymerase

Leiyun Weng [a], Michinori Kohara [b], Takaji Wakita [c], Kunitada Shimotohno [d], Tetsuya Toyoda [a,b,e,*]

[a] Unit of Viral Genome Regulation, Institut Pasteur of Shanghai, Key Laboratory of Molecular Virology & Immunology, Chinese Academy of Sciences, 411 Hefei Road, Shanghai 200025, PR China
[b] Infectious Disease Regulation Project, Tokyo Metropolitan Institute of Medical Sciences, 1-6, Kamikitazawa 2-chome, Setagaya-ku, Tokyo 156-8506, Japan
[c] Department of Virology II, National Institute of Health, 1-23-1 Toyama, Shinjuku, Tokyo 132-8640, Japan
[d] Affiliated Research Institute, Chiba Institute of Technology, 2-17-1 Tsudamuna, Narashino, Chiba 275-0016, Japan
[e] Choju Medical Institute, Fukushimura Hospital, 19-4 Azanakayama, Noyori-cho, Toyohashi, Aichi 441-8124, Japan

ARTICLE INFO

Article history:
Accepted 18 January 2012
Available online 28 January 2012

Keywords:
HCV
NS5B
RNA polymerase
In vitro transcription
Triton X-100
Oligomer

ABSTRACT

Recently, we found that sphingomyelin bound and activated hepatitis C virus (HCV) 1b RNA polymerase (RdRp), thereby recruiting the HCV replication complex into lipid raft structures. Detergents are commonly used for resolving lipids and purifying proteins, including HCV RdRp. Here, we tested the effect of detergents on HCV RdRp activity in vitro and found that non-ionic (Triton X-100, NP-40, Tween 20, Tween 80, and Brij 35) and twitterionic (CHAPS) detergents activated HCV 1b RdRps by 8–16.6 folds, but did not affect 1a or 2a RdRps. The maximum effect of these detergents was observed at around their critical micelle concentrations. On the other hand, ionic detergents (SDS and DOC) completely inactivated polymerase activity at 0.01%. In the presence of Triton X-100, HCV 1b RdRp did not form oligomers, but recruited more template RNA and increased the speed of polymerization. Comparison of polymerase and RNA-binding activity between JFH1 RdRp and Triton X-100-activated 1b RdRp indicated that monomer RdRp showed high activity because JFH1 RdRp was a monomer in physiological conditions of transcription. Besides, 502H plays a key role on oligomerization of 1b RdRp, while 2a RdRps which have the amino acid S at position 502 are monomers. This oligomer formed by 502H was disrupted both by high salt and Triton X-100. On the contrary, HCV 1b RdRp completely lost fidelity in the presence of 0.02% Triton X-100, which suggests that caution should be exercised while using Triton X-100 in anti-HCV RdRp drug screening tests.

1. Introduction

Hepatitis C virus (HCV) belongs to the family *Flaviviridae* and has a positive-stranded RNA genome (Lemon et al., 2007). HCV chronically infects more than 130 million people worldwide (Wasley and Alter, 2000), and infection often induces liver cirrhosis and/or hepatocellular carcinoma (Kiyosawa et al., 1990; Saito et al., 1990). The 9.6-kb-long HCV RNA genome has a long open reading frame encoding a polyprotein of approximately 3,010 amino acids, which is processed into at least 10 viral proteins (NH_2-C-E1-E2-p7-NS2-NS3-NS4A-NS4B-NS5A-NS5B-COOH) by host and viral proteases (Grakoui et al., 1993; Hijikata et al., 1993). The 5′-untranslated region (UTR) contains the internal ribosome entry site (IRES) (Tsukiyama-Kohara et al., 1992). The 3′-UTR contains a poly pyrimidine "U/C" tract, a variable region, and 98-base X-region (Tanaka et al., 1996).

HCV RNA replication depends on the association between the viral protein and raft membranes (Shi et al., 2003; Aizaki et al., 2004), where NS5B RNA polymerase (RdRp) localizes by binding to sphingomyelin (Sakamoto et al., 2005). HCV RdRp is a key enzyme involved in the transcription and replication of the viral genome, and an important target of antivirals. Recently, we found that sphingomyelin bound to and activated HCV 1b RdRp, thereby recruiting the HCV replication complex into lipid raft structures (Weng et al., 2010).

Detergents are commonly used for solubilizing proteins from the lipid-containing components. Some restriction enzymes, reverse transcriptases, and Taq polymerases are stabilized by Triton X-100 or NP-40 (Weyant et al., 1990), while some other polymerases are activated by detergents (Thompson et al., 1972; Wu and Cetta, 1975; Hirschman et al., 1978). Triton X-100 is used for purification of HCV RdRp (Weng et al., 2009). Oligomerization of HCV RdRp is important for its activity (Qin et al., 2002; Clemente-Casares et al., 2011). We have developed an in vitro HCV de novo transcription system by using soluble RdRp and the complementary sequence of the 5′-HCV

Abbreviations: CHAPS, 3-[(3-cholanidopropyl)dimethylammonio]-1-propanesulfonate; CMC, critical micelle concentration; DOC, sodium deoxycholate; HCV, hepatitis C virus; IRES, internal ribosome entry site; KGlu, monopotassium glutamate; PMSF, phenylmethanesulfonyl fluoride; RdRp, RNA polymerase; SDS, sodium dodecyl sulfate; TNTase, terminal nucleotidyl transferase; UTR, untranslated region; nOG, octyl-β-glucoside.

* Corresponding author at: Choju Medical Institute, Fukushimura Hospital, 19-4 Azanakayama, Noyori-cho, Toyohashi, Aichi 441-8124, Japan. Tel.: +81 532 46 7511; fax: +81 532 46 8940.
E-mail address: toyoda_tetsuya@yahoo.co.jp (T. Toyoda).

0378-1119/$ – see front matter © 2012 Elsevier B.V. All rights reserved.
doi:10.1016/j.gene.2012.01.044

genome RNA (SL12-1S template) (Kashiwagi et al., 2002a; Kashiwagi et al., 2002b; Weng et al., 2009; Murayama et al., 2010; Weng et al., 2010). In this paper, we analyzed the effect of detergents on the activity and oligomerization of HCV RdRp, and found that non-ionic (Triton X-100, NP-40, Tween 20, Tween 80, and Brij 35) and twitterionic (3-[(3-cholanidopropyl)dimethylammonio]-1-propanesulfonate [CHAPS]) detergents activated HCV 1b RdRp. In addition, we analyzed the mechanism of RdRp activation by detergents and the relationship between RdRp oligomerization and its activity.

2. Materials and methods

2.1. Mutant HCV RdRp

The H502S mutation of HCR6 (1b) RdRp and the S502H mutation of JFH1 (2a) were introduced using an in vitro mutagenesis kit (Stratagene). Oligonucleotide sequence information is available upon request.

2.2. Purification of HCV RdRp from bacteria

HCV HCR6wt (1b) (Weng et al., 2009), NN (1b) (Watashi et al., 2005), Con1 (1b) (Binder et al., 2007), JFH1wt (2a) (Weng et al., 2009), J6CF (2a) (Murayama et al., 2007), H77 (1a) (Blight et al., 2003), RMT (1a), HCR6 (1b) H502S, and JFH1 (2a) H502S RdRps with a C-terminal 21-amino acid deletion were purified from bacteria as previously described with some modifications (Weng et al., 2009, 2010; Murayama et al., 2010). Briefly, HCV RdRps were eluted from Ni-NTA agarose (Qiagen) with 20 mM Tris–HCl (pH 8.0), 500 mM NaCl, 0.1% Triton X-100, 0.1% 2-mercaptoethanol, and 1 mM phenylmethanesulfonyl fluoride (PMSF) containing 250 mM imidazole after the column was washed with 5 mM imidazole. HCV RdRps were further purified through a Superdex 200 pg column (GE Healthcare) in 20 mM Tris–HCl (pH 8.0), 500 mM NaCl, 1 mM EDTA, 5 mM DTT, 10% glycerol, and 1 mM PMSF to remove contaminating nucleic acids (Fig. S1). The purified HCV RdRps were stored at −80 °C.

2.3. De novo HCV RdRp assay

HCV RdRp assay in the absence of primers was performed as described previously (Weng et al., 2009; Murayama et al., 2010). Briefly, following a 30-min pre-incubation period without ATP, CTP, or UTP, 100 nM HCV RdRp were incubated in 50 mM Tris–HCl (pH 8.0), 200 mM monopotassium glutamate (KGlu), 3.5 mM $MnCl_2$, 1 mM DTT, 0.5 mM GTP, 50 μM ATP, 50 μM CTP, 5 μM [α-^{32}P]UTP, 200 nM 184-nt model RNA template (SL12-1S) (Kashiwagi et al., 2002a; Weng et al., 2009; Murayama et al., 2010), 100 U/ml human placental RNase inhibitor, and the indicated amount of detergent at 29 °C for 90 min. [^{32}P]RNA products were separated in a 6% polyacrylamide gel containing 8 M urea. The resulting autoradiograph was analyzed with a Typhoon Trio Plus image analyzer (GE Healthcare) for the radio activity of 184-nt transcription products.

2.4. Kinetic analysis of HCV RdRp with and without Triton X-100

Kinetic analysis (measurement of *K*m and *V*max) was performed as previously published with and without 0.02% Triton X-100 (Kashiwagi et al., 2002b; Weng et al., 2009). For *K*m and *V*max of ATP, HCV RdRp was incubated in 50, 25, 10, 8, 5, 3, or 1 μM of ATP, 50 μM CTP, 0.5 mM GTP, 5 μM [α-^{32}P]UTP after preincubation in 0.5 mM GTP with and without 0.02% Triton X-100 at 29 °C for 60 min. For *K*m and *V*max of CTP, 50, 25, 10, 8, 5, 3, or 1 μM of CTP, 50 μM ATP, 0.5 mM GTP, and 5 μM [α-^{32}P]UTP, and for *K*m and *V*max of UTP, 50, 25, 10, 8, 5, 3, or 1 μM of UTP, 50 μM ATP, 0.5 mM GTP, 5 μM [α-^{32}P]CTP were used, respectively. For *K*m and *V*max of GTP, HCV RdRp was incubated in 500, 250, 100, 50, 25, 10, or 5 μM of GTP, 50 μM ATP, 50 μM CTP, 5 μM [α-^{32}P]UTP with and without 0.02% Triton X-100 without GTP preincubation.

2.5. Terminal nucleotidyl transferase (TNTase) assay

TNTase assay was performed with the heat denatured 5′-[^{32}P] sym/sub (5′-GAUCGGGCCCGAUC-3′) (Arnold and Cameron, 2000) with 0.5 mM GTP, 50 μM ATP, 50 μM CTP, and 50 μM UTP, and sym/sub with 0.5 mM GTP, 50 μM ATP, 50 μM CTP, and 5 μM [α-^{32}P]-UTP in the same experimental conditions as the above-described transcription assay (Hong et al., 2001). [^{32}P]RNA products were separated in a 15% polyacrylamide gel containing 8 M urea.

2.6. RNA filter-binding assay

RNA filter-binding assays were performed as previously described (Weng et al., 2009). Briefly, 100 nM of HCV RdRp and 100 nM [^{32}P] RNA template (SL12-1S) were incubated with the indicated amount of detergent in 25 μl of 50 mM Tris–HCl (pH 7.5), 200 mM KGlu, 3.5 mM $MnCl_2$, and 1 mM DTT at 29 °C for 30 min. After incubation, the solutions were diluted with 0.5 ml TE and filtered through nitrocellulose membranes (0.45 μm; Millipore). The filter was washed 5 times with TE, and the bound radioisotope was analyzed using the Typhoon Trio Plus image analyzer after being dried.

2.7. Western blot

Western blot analysis using a rabbit anti-HCV RdRp antibody was performed, as described previously (Kashiwagi et al., 2002b).

2.8. Gel filtration

The purified HCR6 (1b), J6CF (2a), and JFH1 (2a) RdRps (50 pmol) were applied on a Superdex 200 pg column in 50 mM Tris–HCl (pH 7.5), 200 mM KGlu or 150 mM NaCl, 3.5 mM $MnCl_2$, 1 mM DTT, and 0.2% glycerol with or without 0.1% Triton X-100.

2.9. Reagents

PMSF, Triton X-100, Tween 20, Tween 80, NP-40, Brij 35, octyl-β-glucoside (nOG), CHAPS, sodium deoxycholate (DOC), and sodium dodecyl sulfate (SDS) were obtained from Amresco; nucleotides were purchased from GE Healthcare; [α-^{32}P]UTP, [α-^{32}P]ATP, [α-^{32}P]GTP, [α-^{32}P]CTP, and [γ-^{32}P]ATP were from New England Nuclear.

2.10. Statistical analysis

Significant differences were determined using the Student's *t*-test.

3. Results

3.1. Effect of detergents on primer-independent HCV RdRp activity

First, we examined the effect of detergents on the primer-independent HCV RdRp activity in vitro (Fig. 1). HCR6 (1b) RdRpwt was activated by all the detergents tests, except octyl-β-glucoside (nOG), but JFH1 (2a) RdRpwt was not. The activation curves of HCR6 (1b) RdRpwt by these detergents plateaued at certain concentrations: 0.002 or 0.004% Triton X-100, 0.001% NP-40, 0.005% Tween 20, 0.001% Tween 80, 0.001% Brij 35, and 0.1% CHAPS. HCR6 (1b) RdRp activity decreased at concentrations greater than 1% Triton X-100, and 30% Triton X-100 completely inhibited HCR6 (1b) RdRpwt activity (Fig. 1A, right panel). With an activation ratio of about 2 at 0.1%, nOG weakly activated HCR6 (1b) RdRpwt. At 0.5% nOG, the

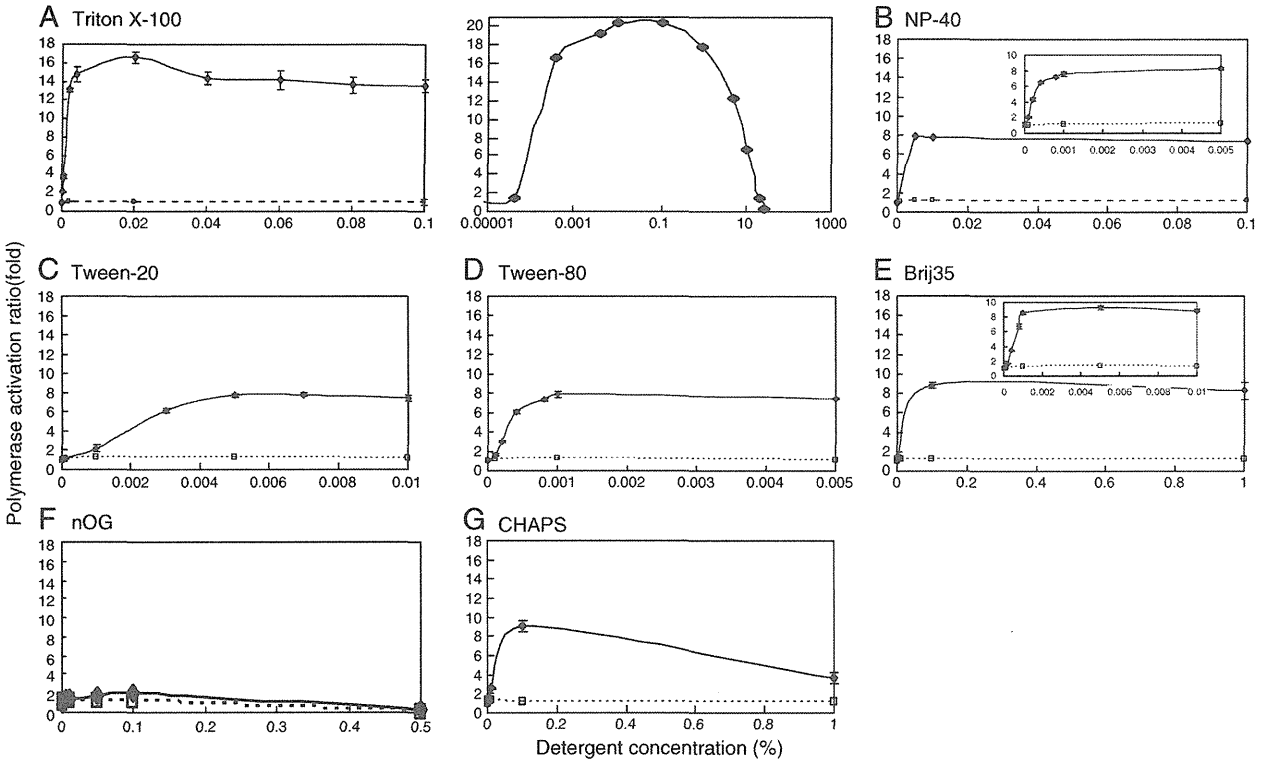

Fig. 1. The effect of detergents on HCV HCR6 and JFH1 RNA polymerases. Wild-type HCR6 (1b) and JFH1 (2a) RdRps were assayed with 0.000004, 0.00004, 0.0004, 0.004, 0.01, 0.02, 0.04, 0.06, 0.08, and 0.1% Triton X-100 (A, left panel); 0.0001, 0.0002, 0.0004, 0.0008, 0.001, 0.005, 0.1, and 0.5% NP-40 (B); 0.0001, 0.001, 0.003, 0.005, 0.007, and 0.01% Tween 20 (C); 0.0001, 0.0002, 0.0004, 0.0008, 0.001, and 0.005% Tween 80 (D); 0.0001, 0.0002, 0.0004, 0.0008, 0.001, 0.005, 0.01, 0.1, and 1% Brij 35 (E); 0.001, 0.005, 0.01, 0.05, and 0.1% nOG (F); or 0.0001, 0.001, 0.005, 0.01, 0.1, 0.1, and 1% CHAPS (G). The effect of high concentration of Triton X-100 on HCR6 (1b) RdRpwt is shown in A (right panel). Inset: Polymerase activation ratio at a lower concentration of NP-40 (B), and Brij 35 (E). Mean and standard deviation (error bar) of the polymerase activation ratio were calculated from 3 independent experiments. The solid line indicates the activation ratio of HCR6 (1b) RdRpwt, and the broken line indicates that of JFH1 (2a) RdRpwt.

activation ratio of HCR6 (1b) RdRpwt was 0.3. At 1% of CHAPS, the activity of HCR6 (1b) RdRpwt was increased by 3.6 folds. The detergent concentration that most activated HCR6 (1b) RdRpwt was approximate to the critical micelle concentration (CMC; Table 1).

When the activation ratios of detergents on HCR6 (1b) RdRpwt were compared, that of Triton X-100 was the highest (Fig. 2, Table 1). Other non-ionic detergents and CHAPS activated HCR6 (1b) RdRpwt to an extent equal to about half of Triton X-100 activation. Although a non-ionic detergent, nOG barely activated HCR6 (1b) RdRpwt.

Because 0.02% Triton X-100 maximally activated HCR6 (1b) RdRpwt, we compared its activation effect on other HCV RdRps (Fig. 3, Table 2). JFH1 (2a) RdRpwt showed the strongest RdRp activity, which is in accordance with previous reports (Weng et al., 2009; Murayama et al., 2010; Schmitt et al., 2011). The RdRp activities of 1b HCR6 and NN activated by Triton X-100 were similar to that of JFH1 RdRpwt in the absence of detergents (Fig. 3B), whereas the RdRp activity of Triton X-100-activated 1b Con1 was about half of that of wild-type JFH1. Neither 1a nor 2a RdRps were activated by Triton X-100.

Table 1
CMC and HCV HCR6 (1b) RdRpwt activation ratio of different detergents.

Detergent	CMC[a] in H_2O (%)	Minimal concentration of maximal activation (%)	Maximal activation (folds)[b]
Triton X-100	0.0155	0.02	16.6 ± 0.56
NP-40	0.0179	0.005	8.3 ± 0.18
Tween 20	0.0074	0.007	7.8 ± 0.21
Tween 80	0.0016	0.001	8.0 ± 0.22
Brij 35	0.1103	0.1	9.2 ± 0.34
nOG	0.672–0.730	0.1	2.1 ± 0.35
CHAPS	0.492–0.615	0.1	9.1 ± 0.60

[a] Modified from "TECHNICAL RESOURCE" (Pierce).
[b] Calculated from Fig. 2.

3.2. RNA template binding with Triton X-100

Next, we compared the template RNA-binding activity of 1a, 1b, and 2a RdRps in the presence of Triton X-100 by using the [^{32}P] SL12-1S model RNA template (Kashiwagi et al., 2002a; Weng et al., 2009, 2010; Murayama et al., 2010) in order to examine the transcription steps activated by Triton X-100 (Fig. 4, Table 2). Template RNA binding was the first step of transcription. The RNA-binding activity of JFH1 RdRpwt was the highest without Triton X-100 (data not shown) (Weng et al., 2009). Different from RdRp activity, the RNA-binding activity of all HCV RdRps was somehow activated by 0.02% Triton X-100. The RNA-binding activity of 1b RdRps was increased by 7–10 folds with Triton X-100.

3.3. Gel filtration of 1b and 2a RdRps

Proteins are generally soluble in detergents. Because HCR6 (1b) RdRpwt showed similar polymerase activity with Triton X-100 as JFH1 (2a) RdRpwt without Triton X-100, we compared the oligomerization state of these RdRps. The oligomerization state of HCR6 (1b) and JFH1 (2a) RdRps under transcription (physiological) conditions (200 mM KGlu or 150 mM NaCl) was analyzed by gel filtration on

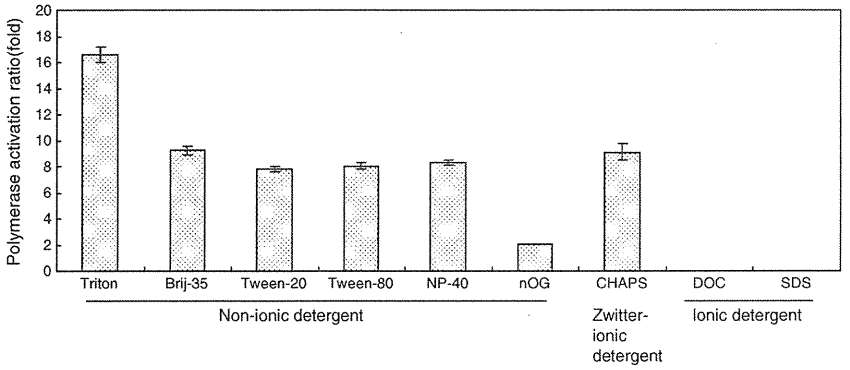

Fig. 2. Activation effect of HCV HCR6 polymerase with detergents at CMC. HCV HCR6 (1b) RdRpwt was assayed at CMC in the presence of Triton X-100 (0.02%), Brij 35 (0.1%), Tween 20 (0.007%), Tween 80 (0.001%), NP40 (0.005%), nOG (0.1%), CHAPS (0.1%), DOC (0.001%), and SDS (0.001%). The activation ratio (fold) is indicated in Table 2. Mean and standard deviation (error bar) of the polymerase activity relative to that without detergent were calculated from 3 independent experiments.

Superdex 200 (Figs. 5 and 6). HCR6 (1b) RdRpwt was eluted from the void volume fraction to the 158-kDa fraction without Triton X-100 (Fig. 5A), which meant that HCR6 (1b) RdRpwt formed random oligomers. It was eluted in the 38-kDa fraction with 0.1% Triton X-100 (Fig. 5B), which indicated that it was smaller than its monomer gel filtration size (Fig. S1D). However, JFH1 (2a) RdRpwt was eluted in the slightly larger fraction (80 kDa) than other HCV RdRps with or without Triton X-100, which indicated the monomer size (Figs. 5C and D, S1F). From the gel filtration and transcription data of HCR6 (1b) RdRpwt and JFH1 (2a) RdRpwt, it was concluded that Triton X-100 dispersed HCR6 (1b) RdRpwt, and that the higher-ordered oligomers of HCR6 (1b) RdRpwt were inactive. Triton X-100 might also affect the interaction between HCR6 (1b) RdRpwt and Superdex200 gel matrix because it was eluted in the smaller molecular weight fractions with Triton X-100 than the monomer gel-filtration size in 0.5 M NaCl (76 kDa, Fig. S1D). Western blot analysis indicated that these RdRp were not degraded (Figs. 5A and B, inset).

Qin et al. found that amino acids 18E and 502H interacted with each other to form the HCV 1b RdRp oligomer/dimer (Qin et al., 2002). Only 2a RdRps harbor the amino acid S at position 502, contrary to other genotype forms of RdRps, which harbor the amino acid H at that same position (Table S1). Therefore, we first examined

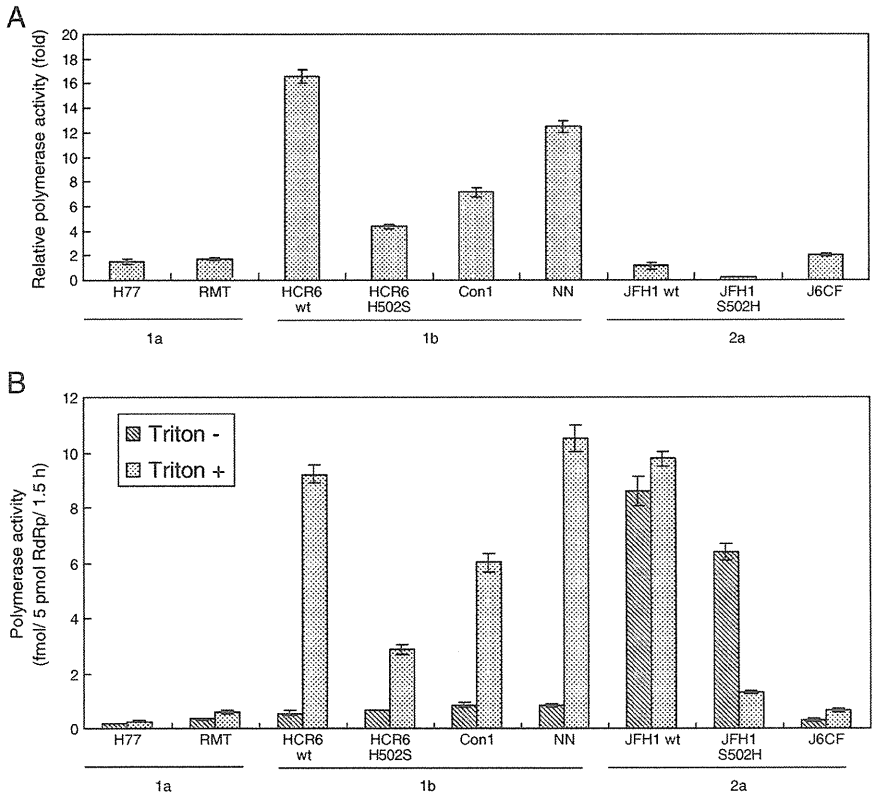

Fig. 3. Effect of 0.02% Triton X-100 on various HCV RNA polymerases. HCV H77 (1a), RMT (1a), HCR6 (1b) wt and H502S, NN (1b), Con1 (1b), JFH1 (2a) wt and S502H, and J6CF (2a) RdRps were assayed in the presence or absence of Triton X-100. A: Activation ratio (fold) of RNA polymerase activity. B: Polymerase activity (fmol of NMP/5 pmol RdRp/1.5 h) in the presence or absence of Triton X-100. Mean and standard deviation (error bar) of the polymerase activity were calculated from 3 independent experiments.

Table 2
Relative activation ratio of HCV RdRp by Triton X-100.

Genotype	1a		1b			2a	
Name	H77	RMT	HCR6	Con1	NN	JFH1	J6CF
Polymerase activity (folds)[a]	1.5 ± 0.17	1.7 ± 0.11	16.6 ± 0.56	7.1 ± 0.38	12.5 ± 0.48	1.1 ± 0.28	2.0 ± 0.12
RNA template-binding activity (folds)[b]	3.8 ± 0.11	3.9 ± 0.18	9.6 ± 0.39	7.9 ± 0.41	6.9 ± 0.16	2.2 ± 0.14	3.4 ± 0.21

[a] Activation ratio of polymerase activity was calculated on the basis of the data represented in Fig. 3A.
[b] Activation ratio of RNA template-binding activity was calculated on the basis of the data represented in Fig. 4A.

another 2a RdRp, J6CF (2a) RdRp, by gel filtration (Fig. 5E). J6CF (2a) RdRp was also eluted as a monomer in 150 mM NaCl buffer without Triton X-100. These gel filtration data was in agreement with the intermolecular interaction and random oligomerization of HCV RdRp caused by 18E and 502E (Qin et al., 2002). Amino acid 18E is shared by HCV RdRps of all 6 genotypes (Table S1) (Clemente-Casares et al., 2011). Therefore, in order to confirm the importance of 502H for oligomerization of HCV RdRp, S502H and H502S mutations were introduced into JFH1 (2a) and HCR6 (1b) RdRps, respectively, and analyzed by gel filtration (Fig. 6). JFH1 (2a) RdRpS502H formed oligomers, and HCR6 (1b) RdRpH502S was eluted in the 15-kDa fraction, which was smaller than its monomeric gel-filtration size. JFH1 (2a) RdRpS502H was eluted around the 50-kDa position with Triton X-100. The RdRp dimers (Qin et al., 2002) were not found in any of our gel filtration profiles. Western blot analysis indicated that the proteins were not degraded (Fig. 6, inset).

The effect of these mutations in RdRp and RNA template-binding activity with and without Triton X-100 was examined (Figs. 3 and 4). JFH1 (2a) RdRpS502H RdRp activity was lower than that of the wild-type in the absence of Triton X-100. Different from the Triton X-100 activation effect on HCR6 (1b) RdRpwt, JFH1 (2a) RdRpS502H RdRp activity decreased, while its RNA template binding increased, in the presence of Triton X-100. HCR6 (1b) RdRpH502S RdRp activity was similar to that of the wild-type, but less activated by Triton X-100 than by the wild-type. RNA template-binding activity of HCR6 (1b) RdRpH502S was activated 2.3 times by Triton X-100.

The 502 mutation data indicated that 502H is important for oligomerization of 1b RdRp molecules in the transcription (physiological salt) condition. Triton X-100 prevented the oligomerization of 1b RdRps by 502H. Moreover, For HCR6 (1b) RdRpwt, the 38-kDa gel filtration molecules (Fig. 5B), which might correspond to the monomer, were more active than the oligomer molecules.

3.4. Fidelity of HCV RdRp with Triton X-100

Finally, we aimed to calculate the kinetic constants (*K*m and *V*max) of HCR6 (1b) RdRp in the presence of 0.02% Triton X-100 because the activation ratio of the polymerase activity was higher than that of RNA binding of HCR6 (1b) RdRp. When nucleotide concentration was low, the amount of product without Triton X-100 decreased; this data can be used to draw Lineweaver–Burk plot (Weng et al., 2009). However, with Triton X-100, the product amount did not decrease according to the decrease of each nucleotide (Fig. 7A). Moreover, each of the nucleotide substrates was removed from the standard HCV in vitro transcription condition (Fig. 7B). Although ATP, CTP or UTP were removed from the reaction buffer, HCV HCR6 (1b) RdRp transcribed the same 184-nt products with Triton X-100, which disappeared without Triton X-100. When GTP was removed, no products were observed with or without Triton X-100 because HCV RdRp required GTP for its structure (Bressanelli et al., 2002). These kinetic experiments indicated that HCV HCR6 (1b) RdRp completely lost fidelity with Triton X-100.

Terminal nucleotidyl transferase (TNTase) activity has been sometimes detected in HCV 1b RdRp preparations (Behrens et al., 1996; Ranjith-Kumar et al., 2001; Ranjith-Kumar et al., 2004; Vo et al., 2004). TNTase activity was not detected in our system, in which the model RNA template contains a CCC-3′ at the 3′-end (Kashiwagi et al., 2002b; Weng et al., 2009). Nevertheless, we examined whether TNTase activity was detected with Triton X-100 using sym/sub, which has GpG-primed transcription activity, but we failed to observe any de novo initiation activity (Hong et al., 2001). No mobility shift was shown by 5′-[^{32}P]sym/sub or sym/sub incubated with [^{32}P]UTP on polyacrylamide gel electrophoresis (PAGE) (Figs. 7C and D), indicating that no TNTase activity was detected in our system with or without Triton X-100.

Apparent *K*m and *V*max of HCR6 (1b) RdRp with Triton X-100 for GTP was 303 ± 15.1 μM and 6.21 ± 0.225/min, respectively (Fig. S3).

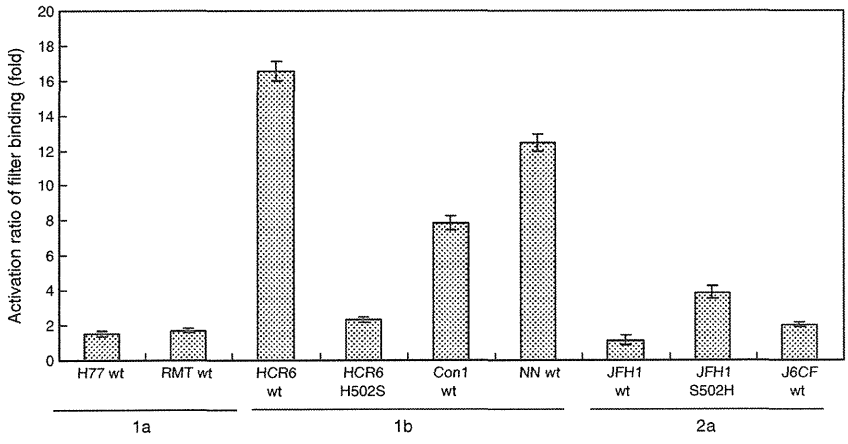

Fig. 4. Effect of 0.02% Triton X-100 on the RNA template-binding activity of HCV RNA polymerases. One hundred nanomolars each of HCV H77 (1a), RMT (1a), HCR6 (1b), NN (1b), Con1 (1b), JFH1 (2a), and J6CF (2a) RdRps with [^{32}P]RNA templates (SL12-1S) were filtered through nitrocellulose membranes after incubation with or without Triton X-100. Mean and standard deviation (error bar) of the RNA filter binding activation (folds) were calculated from 3 independent experiments.

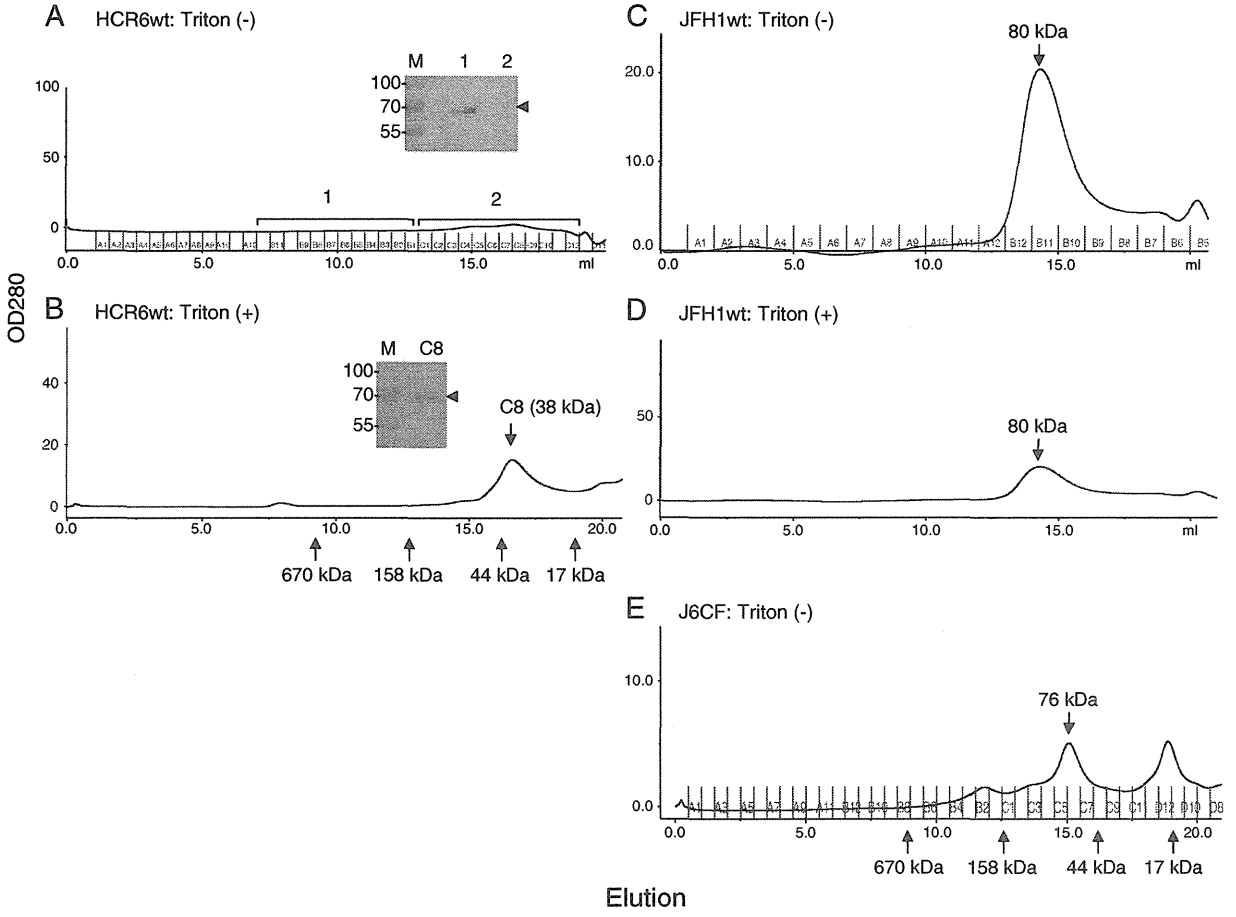

Fig. 5. Superdex 200 gel filtration of HCV HCR6 (1b), JFH1 (2a), and J6CF (2a) wild-type RNA polymerase with or without 0.1% Triton X-100. HCV HCR6 (1b) RdRpwt was applied on Superdex 200 gel filtration columns in 50 mM Tris–HCl (pH 7.5), 150 mM NaCl, 3.5 mM $MnCl_2$, 1 mM DTT, and 0.2% glycerol without (A) or with 0.1% Triton X-100 (B). HCV JFH1 (2a) RdRpwt was applied without (C) or with 0.1% Triton X-100 (D), and J6CF (2a) RdRp was applied without Triton X-100 (E) on the same columns. The elution position of the standard molecular weight markers is indicated below the graph. The molecular weight of the peak fraction is indicated in each graph. Inset in A: The fractions of the void volume—158 kDa (1) and those of lower molecular weight fractions (2) of HCR6 (1b) RdRpwt gel filtration without Triton X-100 were precipitated with TCA and analyzed by western blot. Inset in B: Fraction C8 of HCR6 (1b) RdRpwt with Triton X-100 was precipitated with TCA and analyzed by western blot. The position of HCR6 (1b) RdRpwt is indicated by an arrowhead. The position of the pre-stained size marker is indicated on the left side of the blots.

Km and *Vmax* of HCR6 (1b) RdRp without Triton X-100 for GTP was calculated as 54.7 ± 3.67 μM and 2.52 ± 0.108/min, respectively (Weng et al., 2009).

4. Discussion

Non-ionic (Triton X-100, NP-40, Tween 20, Tween 80, and Brij 35) and twitterionic (CHAPS) detergents activated HCV 1b RdRp by 7.2–16.6 folds when used at their CMC, but did not affect 1a or 2a RdRps (Figs. 1–3, Table 2). In turn, ionic detergents (SDS and DOC) completely inactivated polymerase activity at 0.01%. CMC is the minimum concentration at which a detergent forms micelles; above that concentration, a detergent exists as a large molecular weight complex. The CMC signifies the strength at which a detergent binds to proteins, i.e., low values indicate strong binding, whereas high values indicate weak binding. It is also an indication of the hydrophilicity of a detergent. Triton X-100, NP-40, and Brij 35 at CMC activated Moloney leukemia virus reverse transcriptase by interacting with the hydrophobic domain (Thompson et al., 1972). The activation mechanism of HCV RdRp by these detergents may be similar. However, the detergent interaction domain of HCV RdRp remains to be identified.

Triton X-100 is commonly used for purification of HCV RdRp from the bacteria and insect cells expressing this protein (Lohmann et al., 1997; Luo et al., 2000; Cramer et al., 2006; Weng et al., 2009). HCV 1b RdRp without the C-terminal hydrophobic region expressed in bacteria formed a large molecule complex in 0.1% Triton X-100 or 0.5% CHAPS with a low-salt buffer (<50 mM NaCl) (Qin et al., 2002; Wang et al., 2002). Under low-salt conditions, HCV RdRp was gel filtrated in void volume as a complex with contaminating nucleic acids, because HCV RdRp binds to RNA during purification without high-salt (0.5 M NaCl) stripping (Figs. S1 and S2). Therefore, the presence of HCV 1b RdRp in the void volume fraction of gel filtration by Wang et al. (Wang et al., 2002) could rather represent the complex of HCV RdRp with contaminating nucleic acids. Nevertheless, they also found monomers of HCV 1b RdRp in the gel filtration buffer containing 0.5% CHAPS, which activated polymerase activity (Fig. 1G). Detection of the monomeric HCV 1b RdRps by gel filtration in a buffer containing Triton X-100 and CHAPS has also been reported by other groups (Qin et al., 2002; Wang et al., 2002). HCR6 (1b) RdRpwt formed oligomers in physiological conditions without Triton X-100. In the presence of Triton X-100, HCR6 (1b) RdRpwt was eluted as the monomer which gel-filtration size was smaller than its size in 0.5 M NaCl (Fig. S1D) or calculated from its amino acid composition (64 kDa). HCV 2a (JFH1 and J6CF) RdRps formed a monomer in the same buffer without Triton X-100. Gel filtration analysis of 502 mutants of JFH1 (2a) and HCR6 (1b) RdRps have confirmed that 502H

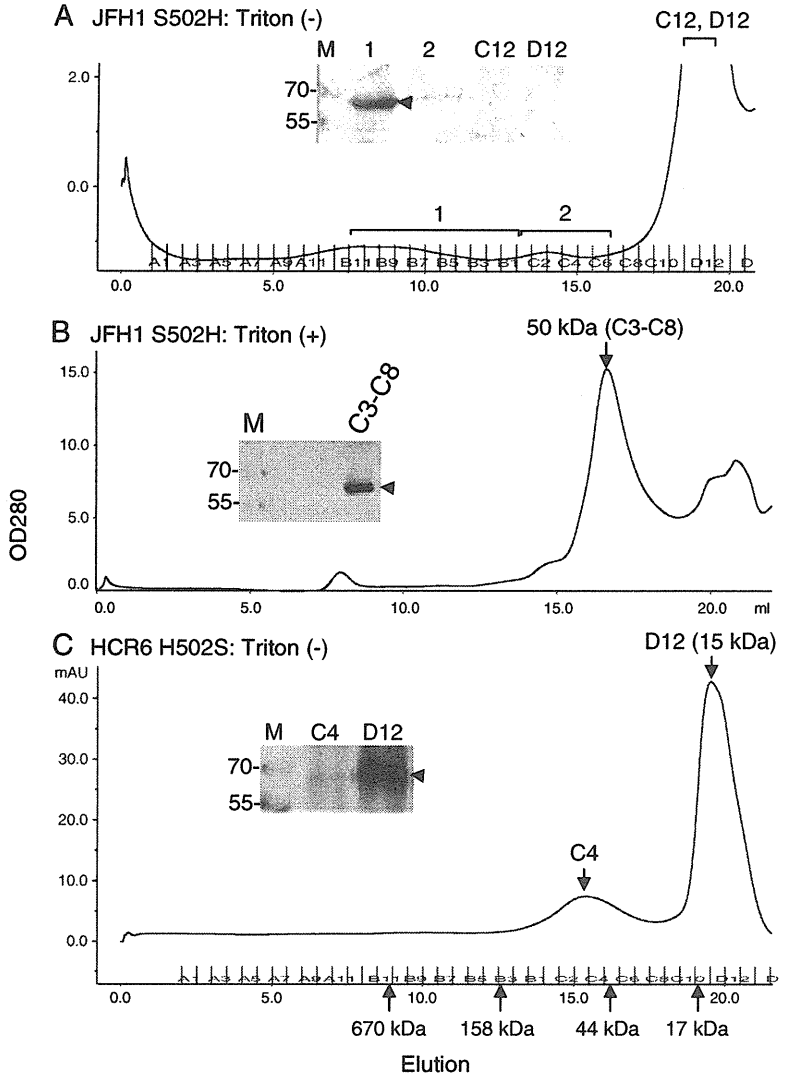

Fig. 6. Superdex 200 gel filtration of HCV JFH1 (2a) and HCR6 (1b) 502 mutant RNA polymerases. JFH1 (2a) S502H (A), and HCR6 (1b) H502S RdRps (C) were applied on Superdex 200 gel filtration columns in 50 mM Tris–HCl (pH 7.5), 150 mM NaCl, 3.5 mM $MnCl_2$, 1 mM DTT, and 0.2% glycerol. JFH1 (2a) RdRpS502H was also applied with 0.1% Triton X-100 (B). Inset in A: The fractions of the void volume—158 kDa (1), those of lower molecular weight fractions (2), fractions C12, and D12 of JFH1 (2a) RdRpS502H gel filtrations were precipitated with TCA and analyzed by western blot. Inset in B: Fraction C3–C8 of JFH1 (2a) RdRpS502H in Triton X-100 were precipitated with TCA and analyzed by western blot. Inset in C: Fractions C4 and D12 of HCR6 (1b) RdRpH502S were precipitated with TCA and analyzed by western blot. The position of HCV RdRp is indicated by an arrowhead. The position of the pre-stained size marker is indicated on the left side of the blots.

is important for the intermolecular interaction of HCV 1b RdRp (Qin et al., 2002). HCV RdRps without the C-terminal hydrophobic domain were soluble in high-salt buffer (>300 mM NaCl; Fig. S1) (Ferrari et al., 1999). The shift to the delayed elution of gel-filtration of HCR6 (1b) RdRpwt and JFH1 (2a) RdRp S502H with Triton X-100, and HCR6 (1b) RdRpH502S may come from the interaction of the RdRps with Superdex200 gel matrix induced by the mutations and Triton X-100.

Our data of HCV RdRp oligomerization at 502H (Fig. 6) are in agreement with those by Qin et al. (Qin et al., 2002), but are contradictory to those obtained by more sensitive methods (fluorescence resonance energy transfer [FRET] and yeast two-hybrid system) (Wang et al., 2002; Clemente-Casares et al., 2011). Interactions between a charged amino acid (His) and an aromatic residue (Trp) (Fernandez-Recio et al., 1997; Matthews et al., 1997; Takeuchi et al., 2003), or His–Glu interactions (Marti and Bosshard, 2003), are often found in proteins. JFH1 (2a) RdRpwt did not form dimers (Chinnaswamy et al., 2010). 502H may interact with 125 W in αF (Clemente-Casares et al., 2011), but not with 18E (Qin et al., 2002). This interaction is dissociated both with high-salt (Fig. S1) and with Triton X-100 (Figs. 5 and 6). Taken together, 502H of HCV 1b RdRp is important for oligomer formation in transcription (physiological salt) conditions. Besides the oligomerization using 502H, the αF and αT helixes of HCV RdRp, which were proposed to be involved in oligomerization (Clemente-Casares et al., 2011), may also be involved in oligomerization of the molecules in transcription condition. The 502 mutations in HCR6 (1b) and JFH1 (2a) RdRps are likely to affect the structure of the template channel by affecting the helix structures of the thumb domain (Bressanelli et al., 2002; Chinnaswamy et al., 2008) because the polymerase and RNA template binding activity of these mutant RdRps was not activated by Triton X-100 (Figs. 3 and 4). These findings indicate the importance around amino acid 502H for HCV 1b RdRp structure. However, these data contradict to the previous reports (Qin et al., 2002; Clemente-Casares et al., 2011).

Comparing the polymerase and template RNA-binding activity of JFH1 (2a) and HCR6 (1b) RdRps with and without Triton X-100,

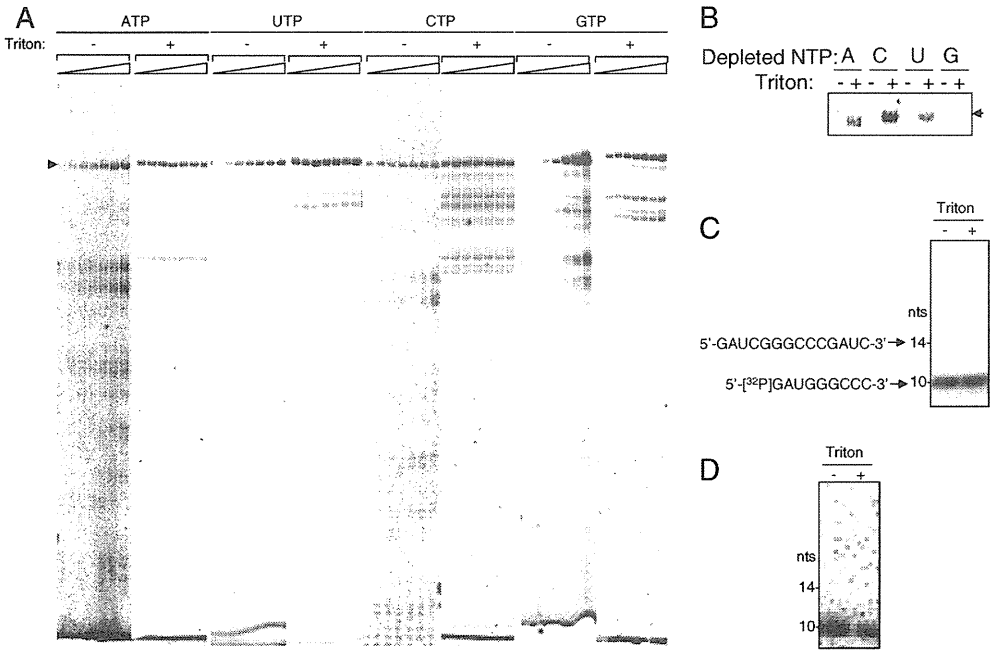

Fig. 7. Effect of substrate concentrations on in vitro transcription of HCR6 (1b) wild-type RNA polymerase, and TNTase activity in the presence of Triton X-100. A: Effect of nucleotide concentration on HCV HCR6 (1b) RdRpwt in vitro transcription with (+) and without (−) 0.02% Triton X-100. The concentration of ATP, UTP, and CTP varied from 1 to 50 μM, and that of GTP varied from 5 to 500 μM. B: Effect of nucleotide depletion on HCV HCR6 (1b) RdRpwt in vitro transcription with (+) and without (−) 0.02% Triton X-100. The position of 184-nt products is indicated by an arrowhead (A and B). C: TNTase activity of HCV HCR6 (1b) RdRpwt. 5′-[^{32}P]sym/sub was transcribed by HCV HCR6 (1b) RdRpwt with (+) and without (−) 0.02% Triton X-100. D: TNTase activity of HCV HCR6 (1b) RdRpwt. sym/sub was transcribed with [^{32}P]UTP by HCV HCR6 (1b) RdRpwt with (+) and without (−) 0.02% Triton X-100. The position of 10-nt sym/sub and 14-nt is indicated on the left.

RdRp which formed oligomer using 502H did not show high polymerase activity (Figs. 3–6). The inactive oligomer may be a part of the reason why a small fraction, less than 1%, of the purified HCV BK RdRp which belonged to 1b participated productively in transcription in vitro (Carroll et al., 2000). Taking together the data obtained by FRET (Clemente-Casares et al., 2011) and yeast two-hybrid systems (Wang et al., 2002), dynamic intermolecular interactions may occur under transcription conditions through the αT helix where amino acid 502 is located. The reason why only 1b RdRp was activated with Triton X-100 although RNA binding of all the RdRps tested was enhanced with Triton X-100, is not clear.

In case of JFH1 (2a) RdRp, the interaction with Triton X-100 may be different from that of HCR6 (1b) RdRp because it was not activated with Triton X-100 (Figs. 1 and 3), and because its gel-filtration profile was not affected with Triton X-100 (Fig. 5). This may be the reason of the inhibition of polymerase activity of JFH1 (2a) RdRpS502H by Triton X-100 although it was also disrupted to monomer (Figs. 3 and 6).

Triton X-100 activated only HCV 1b RdRp (Figs. 3 and 4). The closed conformation of HCV RdRp is required for de novo initiation (Chinnaswamy et al., 2008). With and without Triton X-100, JFH1 (2a) RdRpwt showed as high polymerase activity as HCR6 (1b) RdRpwt did with Triton X-100 (Fig. 3B). The very closed conformation of JFH1 (2a) RdRp is proposed to facilitate de novo initiation and high polymerase activity (Simister et al., 2009). Triton X-100 may also help the conformational change of HCR6 (1b) RdRp to the very closed conformation like that of JFH1 (2a) RdRp during transcription initiation.

HCV RdRp was co-purified with nucleic acids (Figs. S1 and S2). The contaminating nucleic acids were removed from HCV RdRp by high salt treatment. The contaminating nucleic acids carry proteins that have affinity to them, which misleads HCV in vitro transcription data. They also oligomerize HCV RdRp by crosslinking them. In a similar way, the contaminating nucleic acids in HCV RdRp preparations may mislead the binding data of HCV RdRp with other proteins.

From the activation kinetics of the detergents (Fig. 1, Table 1), the polymerase activation of 1b RdRp is likely to depend on the micelle formation of the detergent and on the direct interaction between RdRp and the detergents. The reason why the non-ionic detergent nOG did not activate the HCV RdRp is not known (Figs. 1 and 2).

The interaction mechanism of Triton X-100 and HCV 1b RdRp may be similar as that of sphingomyelin and HCV 1b RdRp because their activation kinetics were similar and the activated genotype was the same (Weng et al., 2010). Sphingomyelin activated only HCV 1b, but did not activate 1a or 2a RdRps. Both the activation curve of sphingomyelin and that of Triton X-100 showed the linear increase of polymerase activity. Then, sphingomyelin reached plateau at 20 molecules, and Triton X-100 reached plateau around its CMC.

Data about TNTase activity of HCV RdRp are controversial (Behrens et al., 1996; Ranjith-Kumar et al., 2001, 2004; Vo et al., 2004). In our system, TNTase activity was not detected with or without Triton X-100 (Figs. 7C and D).

GTP binds to HCV RdRp both as substrate and as a component of RdRp (Bressanelli et al., 2002). The apparent *Km* for GTP with Triton X-100 indicated that the substrate affinity dropped as low as to lose fidelity (Table 1, Figs. 7A and B). Triton X-100 may have affected the substrate-binding although its mechanism is not clear. HCV 1b full-length RdRp transcription activity obtained with CHAPS (Wang et al., 2002) might be that without fidelity as shown with Triton X-100. Detergents should not be used while screening substrate inhibitors of HCV RdRp. These data indicate that caution should be exercised while using detergents in anti-HCV RdRp drug screening tests.

Supplementary materials related to this article can be found online at doi:10.1016/j.gene.2012.01.044.

Acknowledgments

We thank Dr. J. Bukh, Dr. C. Rice, and Dr. R. Bartenshlager for providing pJ6CF, pHCVrepl3(S2204I)Neo, and Con1, respectively. This

work was supported by a Grant-in-Aid from the Chinese Academy of Sciences (O514P51131 and KSCX1-YW-10), the Chinese 973 Project (2009CB522504), and the Chinese National Science and Technology Major Project (2008ZX10002-014).

References

Aizaki, H., Lee, K.J., Sung, V.M., Ishiko, H., Lai, M.M., 2004. Characterization of the hepatitis C virus RNA replication complex associated with lipid rafts. Virology 324, 450–461.

Arnold, J.J., Cameron, C.E., 2000. Poliovirus RNA-dependent RNA polymerase (3D(pol)). Assembly of stable, elongation-competent complexes by using a symmetrical primer-template substrate (sym/sub). J. Biol. Chem. 275, 5329–5336.

Behrens, S.E., Tomei, L., De Francesco, R., 1996. Identification and properties of the RNA-dependent RNA polymerase of hepatitis C virus. EMBO J. 15, 12–22.

Binder, M., Quinkert, D., Bochkarova, O., Klein, R., Kezmic, N., Bartenschlager, R., Lohmann, V., 2007. Identification of determinants involved in initiation of hepatitis C virus RNA synthesis by using intergenotypic replicase chimeras. J. Virol. 81, 5270–5283.

Blight, K.J., McKeating, J.A., Marcotrigiano, J., Rice, C.M., 2003. Efficient replication of hepatitis C virus genotype 1a RNAs in cell culture. J. Virol. 77, 3181–3190.

Bressanelli, S., Tomei, L., Rey, F.A., De Francesco, R., 2002. Structural analysis of the hepatitis C virus RNA polymerase in complex with ribonucleotides. J. Virol. 76, 3482–3492.

Carroll, S.S., Sardana, V., Yang, Z., Jacobs, A.R., Mizenko, C., Hall, D., Hill, L., Zugay-Murphy, J., Kuo, L.C., 2000. Only a small fraction of purified hepatitis C RNA-dependent RNA polymerase is catalytically competent: implications for viral replication and in vitro assays. Biochemistry 39, 8243–8249.

Chinnaswamy, S., Murali, A., Li, P., Fujisaki, K., Kao, C.C., 2010. Regulation of de novo-initiated RNA synthesis in hepatitis C virus RNA-dependent RNA polymerase by intermolecular interactions. J. Virol. 84, 5923–5935.

Chinnaswamy, S., Yarbrough, I., Palaninathan, S., Kumar, C.T., Vijayaraghavan, V., Demeler, B., Lemon, S.M., Sacchettini, J.C., Kao, C.C., 2008. A locking mechanism regulates RNA synthesis and host protein interaction by the hepatitis C virus polymerase. J. Biol. Chem. 283, 20535–20546.

Clemente-Casares, P., Lopez-Jimenez, A.J., Bellon-Echeverria, I., Encinar, J.A., Martinez-Alfaro, E., Perez-Flores, R., Mas, A., 2011. De novo polymerase activity and oligomerization of hepatitis C virus RNA-dependent RNA-polymerases from genotypes 1 to 5. PLoS One 6, e18515.

Cramer, J., Jaeger, J., Restle, T., 2006. Biochemical and pre-steady-state kinetic characterization of the hepatitis C virus RNA polymerase (NS5BDelta21, HC-J4). Biochemistry 45, 3610–3619.

Fernandez-Recio, J., Vazquez, A., Civera, C., Sevilla, P., Sancho, J., 1997. The tryptophan/histidine interaction in alpha-helices. J. Mol. Biol. 267, 184–197.

Ferrari, E., Wright-Minogue, J., Fang, J.W., Baroudy, B.M., Lau, J.Y., Hong, Z., 1999. Characterization of soluble hepatitis C virus RNA-dependent RNA polymerase expressed in *Escherichia coli*. J. Virol. 73, 1649–1654.

Grakoui, A., McCourt, D.W., Wychowski, C., Feinstone, S.M., Rice, C.M., 1993. Characterization of the hepatitis C virus-encoded serine proteinase: determination of proteinase-dependent polyprotein cleavage sites. J. Virol. 67, 2832–2843.

Hijikata, M., Mizushima, H., Tanji, Y., Komoda, Y., Hirowatari, Y., Akagi, T., Kato, N., Kimura, K., Shimotohno, K., 1993. Proteolytic processing and membrane association of putative nonstructural proteins of hepatitis C virus. Proc. Natl. Acad. Sci. U. S. A. 90, 10773–10777.

Hirschman, S.Z., Gerber, M., Garfinkel, E., 1978. Differential activation of hepatitis B DNA polymerase by detergent and salt. J. Med. Virol. 2, 61–76.

Hong, Z., Cameron, C.E., Walker, M.P., Castro, C., Yao, N., Lau, J.Y., Zhong, W., 2001. A novel mechanism to ensure terminal initiation by hepatitis C virus NS5B polymerase. Virology 285, 6–11.

Kashiwagi, T., Hara, K., Kohara, M., Iwahashi, J., Hamada, N., Honda-Yoshino, H., Toyoda, T., 2002a. Promoter/origin structure of the complementary strand of hepatitis C virus genome. J. Biol. Chem. 277, 28700–28705.

Kashiwagi, T., Hara, K., Kohara, M., Kohara, K., Iwahashi, J., Hamada, N., Yoshino, H., Toyoda, T., 2002b. Kinetic analysis of C-terminally truncated RNA-dependent RNA polymerase of hepatitis C virus. Biochem. Biophys. Res. Commun. 290, 1188–1194.

Kiyosawa, K., Sodeyama, T., Tanaka, E., Gibo, Y., Yoshizawa, K., Nakano, Y., Furuta, S., Akahane, Y., Nishioka, K., Purcell, R.H., et al., 1990. Interrelationship of blood transfusion, non-A, non-B hepatitis and hepatocellular carcinoma: analysis by detection of antibody to hepatitis C virus. Hepatology 12, 671–675.

Lemon, S., Walker, C., Alter, M., Yi, M., 2007. Hepatitis C virus. In: Knipe, D., Howley, P. (Eds.), *Fields Virology*. Lippincott-Raven Publishers, Philadelphia, PA, pp. 1253–1304.

Lohmann, V., Korner, F., Herian, U., Bartenschlager, R., 1997. Biochemical properties of hepatitis C virus NS5B RNA-dependent RNA polymerase and identification of amino acid sequence motifs essential for enzymatic activity. J. Virol. 71, 8416–8428.

Luo, G., Hamatake, R.K., Mathis, D.M., Racela, J., Rigat, K.L., Lemm, J., Colonno, R.J. De, 2000. novo initiation of RNA synthesis by the RNA-dependent RNA polymerase (NS5B) of hepatitis C virus. J. Virol. 74, 851–863.

Marti, D.N., Bosshard, H.R., 2003. Electrostatic interactions in leucine zippers: thermodynamic analysis of the contributions of Glu and His residues and the effect of mutating salt bridges. J. Mol. Biol. 330, 621–637.

Matthews, J.M., Ward, L.D., Hammacher, A., Norton, R.S., Simpson, R.J., 1997. Roles of histidine 31 and tryptophan 34 in the structure, self-association, and folding of murine interleukin-6. Biochemistry 36, 6187–6196.

Murayama, A., Date, T., Morikawa, K., Akazawa, D., Miyamoto, M., Kaga, M., Ishii, K., Suzuki, T., Kato, T., Mizokami, M., Wakita, T., 2007. The NS3 helicase and NS5B-to-3′X regions are important for efficient hepatitis C virus strain JFH-1 replication in Huh7 cells. J. Virol. 81, 8030–8040.

Murayama, A., Weng, L., Date, T., Akazawa, D., Tian, X., Suzuki, T., Kato, T., Tanaka, Y., Mizokami, M., Wakita, T., Toyoda, T., 2010. RNA polymerase activity and specific RNA structure are required for efficient HCV replication in cultured cells. PLoS Pathog. 6, e1000885.

Qin, W., Luo, H., Nomura, T., Hayashi, N., Yamashita, T., Murakami, S., 2002. Oligomeric interaction of hepatitis C virus NS5B is critical for catalytic activity of RNA-dependent RNA polymerase. J. Biol. Chem. 277, 2132–2137.

Ranjith-Kumar, C.T., Gajewski, J., Gutshall, L., Maley, D., Sarisky, R.T., Kao, C.C., 2001. Terminal nucleotidyl transferase activity of recombinant Flaviviridae RNA-dependent RNA polymerases: implication for viral RNA synthesis. J. Virol. 75, 8615–8623.

Ranjith-Kumar, C.T., Sarisky, R.T., Gutshall, L., Thomson, M., Kao, C.C. De, 2004. novo initiation pocket mutations have multiple effects on hepatitis C virus RNA-dependent RNA polymerase activities. J. Virol. 78, 12207–12217.

Saito, I., Miyamura, T., Ohbayashi, A., Harada, H., Katayama, T., Kikuchi, S., Watanabe, Y., Koi, S., Onji, M., Ohta, Y., et al., 1990. Hepatitis C virus infection is associated with the development of hepatocellular carcinoma. Proc. Natl. Acad. Sci. U. S. A. 87, 6547–6549.

Sakamoto, H., Okamoto, K., Aoki, M., Kato, H., Katsume, A., Ohta, A., Tsukuda, T., Shimma, N., Aoki, Y., Arisawa, M., Kohara, M., Sudoh, M., 2005. Host sphingolipid biosynthesis as a target for hepatitis C virus therapy. Nat. Chem. Biol. 1, 333–337.

Schmitt, M., Scrima, N., Radujkovic, D., Caillet-Saguy, C., Simister, P.C., Friebe, P., Wicht, O., Klein, R., Bartenschlager, R., Lohmann, V., Bressanelli, S., 2011. A comprehensive structure-function comparison of hepatitis C virus strain JFH1 and J6 polymerases reveals a key residue stimulating replication in cell culture across genotypes. J. Virol. 85, 2565–2581.

Shi, S.T., Lee, K.J., Aizaki, H., Hwang, S.B., Lai, M.M., 2003. Hepatitis C virus RNA replication occurs on a detergent-resistant membrane that cofractionates with caveolin-2. J. Virol. 77, 4160–4168.

Simister, P., Schmitt, M., Geitmann, M., Wicht, O., Danielson, U.H., Klein, R., Bressanelli, S., Lohmann, V., 2009. Structural and functional analysis of hepatitis C virus strain JFH1 polymerase. J. Virol. 83, 11926–11939.

Takeuchi, H., Okada, A., Miura, T., 2003. Roles of the histidine and tryptophan side chains in the M2 proton channel from influenza A virus. FEBS Lett. 552, 35–38.

Tanaka, T., Kato, N., Cho, M.J., Sugiyama, K., Shimotohno, K., 1996. Structure of the 3′ terminus of the hepatitis C virus genome. J. Virol. 70, 3307–3312.

Thompson, F.M., Libertini, L.J., Joss, U.R., Calvin, M., 1972. Detergent effects on a reverse transcriptase activity and on inhibition by rifamycin derivatives. Science 178, 505–507.

Tsukiyama-Kohara, K., Iizuka, N., Kohara, M., Nomoto, A., 1992. Internal ribosome entry site within hepatitis C virus RNA. J. Virol. 66, 1476–1483.

Vo, N.V., Tuler, J.R., Lai, M.M., 2004. Enzymatic characterization of the full-length and C-terminally truncated hepatitis C virus RNA polymerases: function of the last 21 amino acids of the C terminus in template binding and RNA synthesis. Biochemistry 43, 10579–10591.

Wang, Q.M., Hockman, M.A., Staschke, K., Johnson, R.B., Case, K.A., Lu, J., Parsons, S., Zhang, F., Rathnachalam, R., Kirkegaard, K., Colacino, J.M., 2002. Oligomerization and cooperative RNA synthesis activity of hepatitis C virus RNA-dependent RNA polymerase. J. Virol. 76, 3865–3872.

Wasley, A., Alter, M.J., 2000. Epidemiology of hepatitis C: geographic differences and temporal trends. Semin. Liver Dis. 20, 1–16.

Watashi, K., Ishii, N., Hijikata, M., Inoue, D., Murata, T., Miyanari, Y., Shimotohno, K., 2005. Cyclophilin B is a functional regulator of hepatitis C virus RNA polymerase. Mol. Cell 19, 111–122.

Weng, L., Du, J., Zhou, J., Ding, J., Wakita, T., Kohara, M., Toyoda, T., 2009. Modification of hepatitis C virus 1b RNA polymerase to make a highly active JFH1-type polymerase by mutation of the thumb domain. Arch. Virol. 154, 765–773.

Weng, L., Hirata, Y., Arai, M., Kohara, M., Wakita, T., Watashi, K., Shimotohno, K., He, Y., Zhong, J., Toyoda, T., 2010. Sphingomyelin activates hepatitis C virus RNA polymerase in a genotype specific manner. J. Virol. 84, 11761–11770.

Weyant, R.S., Edmonds, P., Swaminathan, B., 1990. Effect of ionic and nonionic detergents on the Taq polymerase. Biotechniques 9, 308–309.

Wu, A.M., Cetta, A., 1975. On the stimulation of viral DNA polymerase activity by nonionic detergent. Biochemistry 14, 789–795.

SCIENTIFIC REPORTS

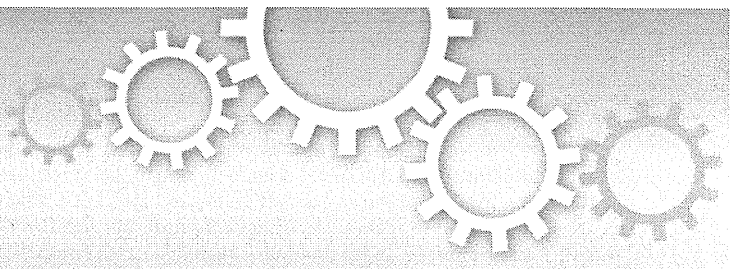

OPEN

SUBJECT AREAS:
GENE REGULATION
VIROLOGY
PATHOGENS
RNAI

Received
7 November 2011

Accepted
23 January 2012

Published
10 February 2012

Correspondence and requests for materials should be addressed to M.S. (sudomsy@chugai-pharm.co.jp)

An orally available, small-molecule interferon inhibits viral replication

Hideyuki Konishi[1], Koichi Okamoto[1], Yusuke Ohmori[1], Hitoshi Yoshino[2], Hiroshi Ohmori[1], Motooki Ashihara[1], Yuichi Hirata[3], Atsunori Ohta[1], Hiroshi Sakamoto[1], Natsuko Hada[1], Asao Katsume[1], Michinori Kohara[3], Kazumi Morikawa[2], Takuo Tsukuda[1], Nobuo Shimma[1], Graham R. Foster[4], William Alazawi[4], Yuko Aoki[1], Mikio Arisawa[1] & Masayuki Sudoh[1]

[1]Kamakura Research Laboratories, Chugai Pharmaceutical Co. Ltd., Kamakura, Kanagawa, Japan, [2]Fuji-Gotemba Research Laboratories, Chugai Pharmaceutical Co. Ltd., Gotemba, Shizuoka, Japan, [3]Department of Microbiology and Cell Biology, The Tokyo Metropolitan Institute of Medical Science, Setagaya-ku, Tokyo, Japan, [4]Queen Mary University of London, Blizard Institute of Cellular and Molecular Science, 4 Newark Street, London E1 4AT, UK.

Most acute hepatitis C virus (HCV) infections become chronic and some progress to liver cirrhosis or hepatocellular carcinoma. Standard therapy involves an interferon (IFN)-α-based regimen, and efficacy of therapy has been significantly improved by the development of protease inhibitors. However, several issues remain concerning the injectable form and the side effects of IFN. Here, we report an orally available, small-molecule type I IFN receptor agonist that directly transduces the IFN signal cascade and stimulates antiviral gene expression. Like type I IFN, the small-molecule compound induces IFN-stimulated gene (ISG) expression for antiviral activity *in vitro* and *in vivo* in mice, and the ISG induction mechanism is attributed to a direct interaction between the compound and IFN-α receptor 2, a key molecule of IFN-signaling on the cell surface. Our study highlights the importance of an orally active IFN-like agent, both as a therapy for antiviral infections and as a potential IFN substitute.

Hepatitis C virus (HCV) infection affects 170 million people worldwide[1], and most acute HCV infections become chronic, with some progression to liver cirrhosis or hepatocellular carcinoma. HCV has a plus-strand RNA genome that encodes both structural proteins and the nonstructural (NS) proteins 2, 3, 4A, 4B, 5A and 5B. Current standard therapy against chronic HCV infection includes the use of host factor-targeting pegylated interferon (PEG-IFN)-α and ribavirin[2], which is effective in only 50% of patients chronically infected with HCV genotype 1[3]. The main causes of this low rate of efficacy may be (i) single-nucleotide polymorphisms (SNPs) in the upstream region of the *IL28B* gene and (ii) low compliance with the therapy, which must be administered subcutaneously. Regarding the first cause—SNPs—the host factors that are important in the early response to therapy remain unknown. However, recent studies report that genetic variants near *IL28B*, which encodes IFN-λ3 (interleukin 28B), correlate with the response to treatment of chronic hepatitis C infection using IFN-α/ribavirin combination therapy[4–7]. Patients with an rs12979860 SNP genotype of CC are reported to have a stronger response to IFN therapy (up to an 80% sustained virological response (SVR) rate with the combined therapy) than those with TC or TT genotypes[4]. Regarding the lack of compliance, the current therapy using recombinant IFN is a weekly injectable formulation that is unstable, requires refrigeration, and is expensive and complex to administer. Furthermore, therapy is often poorly tolerated as a result of the presence of many adverse effects, including flu-like symptoms, hematological abnormalities and adverse neuropsychiatric events, any of which may require early discontinuation[8]. These side effects may result in dose modifications that lead to less-than-optimal responses.

Recent trends in drug development focus on drugs targeted against viral proteins such as NS 3/4A serine protease, RNA helicase, NS4B, NS5A, and NS5B RNA-dependent RNA polymerase[9]. Very recently, two NS3/4A protease inhibitors, telaprevir and boceprevir, have been approved as new anti-HCV agents. Adding such an inhibitor to the standard therapy in the ADVANCE[10] and the SPRINT-2[11] trials achieved significantly higher SVR rates, but the issue still remains that using these inhibitors without injectable IFN possibly yields clinical resistance[12]. To overcome this problem and alleviate the low compliance outlined above, an orally available IFN would be valuable because the dosing regimen is less complex.

IFNs induce the expression of a subset of IFN-stimulated genes (ISG)[13], some of which show antiviral activity or are involved in lipid metabolism, apoptosis, protein degradation and inflammation[14]. IFNs are not only effective

against HCV infection, but are also essential for innate immunity. Broadly speaking, type I IFNs (IFN-α and -β) bind to their receptor, causing the phosphorylation and activation of JAK1 and Tyk2, which is followed by the phosphorylation of signal transducers and activators of transcription (STATs) and subsequent ISG expression. To activate the JAK/STAT pathway, IFN-α requires the IFN-α/β receptor, which consists of 2 subunits, IFN-α receptor (IFNAR) 1 and IFNAR2. These IFNAR subunits together form a heterodimer upon IFN stimulation. This association of IFNAR2 and IFNAR1 is required to mediate the antiviral, antiproliferative, and apoptotic effects of type I IFNs[15–17] because the dimerization of IFNARs induces the phosphorylation of the receptor-associated tyrosine kinases, JAK1 and Tyk2, and the phosphorylated JAK kinases then phosphorylate STAT1 and STAT2. In turn, phosphorylated STAT1 and STAT2 bind to IRF9 to form the transcriptional activator IFN-stimulating gene factor 3 (ISGF3) that induces the expression of a subset of ISGs[13].

Using quantitative high-throughput screening (HTS), we identified in this study a novel small molecule that acts like IFN by directly interacting with the type I IFN receptor to drive ISG expression. Our results indicate that oral administration of the small-molecule IFN agonist stimulates ISG expression in mice, and that the ISG expression from this small-molecule IFN provides antiviral activity, indicating that the compound may be a potential therapeutic IFN substitute.

Results

Identification of antiviral small-molecule IFN agonists by high-throughput chemical library screening. HCV replicon cells, which were established ten years ago[18] using a cell line that expresses the HCV genotype 1b subgenomic replicon[19], possess a luciferase gene as a reporter optimized for use in a robust HTS system. The HTS system provides in-depth analysis of primary screening results, including detailed information regarding potency, efficacy and structure-activity relationships. IFNs show strong inhibition using this system and have been used as a positive control in the assay. Many compounds, including HCV protease inhibitors and HCV polymerase nucleoside/non-nucleoside analogs, have been assessed and are being developed for clinical testing. Analysis of data from the combination of target/counterscreen HTS, data from other assays measuring cellular toxicity, *in vitro* sphingolipid biosynthesis and HCV enzymatic activity (including protease and polymerase) allowed us to select compounds with potentially novel modes of action from the primary screen.

A secondary IFN signal assay, using a luciferase reporter gene which was located downstream of the IFN-stimulated response element (ISRE), eliminated assay-related false-positive compounds. Of the remaining anti-HCV replicon compounds, one of the most active was an imidazonaphthyridine with the structural formula 8-(1, 3, 4-oxadiazol-2-yl)-2, 4-bis (trifluoromethyl) imidazo [1, 2-a] [1, 8] naphthyridine (RO4948191, hereinafter RO8191) (Fig. 1a). This compound strongly suppressed HCV replicon activity at 72 h in a dose-dependent manner (Fig. 1b, left graph) without inducing host cell toxicity, as measured by the WST-8 (Fig. 1b, right graph) and CellTiter-Glo assays (data not shown). The IC_{50} (50% inhibitory concentration) of the compound in an anti-HCV replicon assay was 200 nM. The compound suppressed viral replication within 24 h and showed even more effective inhibition, without cytotoxicity, after 7 days (Supplementary Fig. 1). In addition, the HCV RNA replicon levels significantly decreased after incubation with the compound for 72 h, as determined by real-time reverse transcription (RT)-polymerase chain reaction (PCR) analysis (Fig. 1c). Immunostaining showed that levels of the proteins HCV NS3 and NS4A, which are localized mainly in the perinuclear region of the replicon cells, were also reduced after RO8191 treatment for 24 h (Fig. 1d). This treatment also resulted in the disappearance of viral proteins such as NS3, NS4A/B, and NS5A/B, as shown by western blot analysis (Fig. 1e). The luciferase activity of HCV subgenomic genotype 2 replicon cells (JFH1, data not shown) and, surprisingly, the HCV viral titer of JFH1[20] in a Huh-7/K4 cell line were also reduced by RO8191 treatment (Fig. 1f).

RO8191 induces IFN signals, ISGs expression and JAK/STAT phosphorylation. To clarify whether RO8191 shows inhibitory activity against another RNA virus, we tested its action in encephalomyocarditis virus (EMCV)-infected A549 cells. RO8191 showed a cell-protective activity against EMCV infection similar to that of IFN-α (Fig. 2a). Because IFN-α is the most common host cell factor to exert its antiviral activity against HCV[21,22] by inducing ISG expression[13], we compared the gene expression profiles of IFN-α and RO8191 by conducting a global-scale DNA microarray analysis to identify genes, especially ISGs[23], that were regulated by RO8191. As expected, RO8191 increased the expression of some ISGs (Supplementary Fig. 2 and Supplementary Table 1). DNA microarray analysis showed that RO8191 induced the expression of IP-10 (CXCL10), known as an ISG, RO8191 did not induce the genes encoding inflammatory cytokines and chemokines (Supplementary Fig. 3a). And, a reporter gene assay was performed using an NF-κB reporter gene. We transiently transfected the reporter gene to HCV-naïve HuH-7 cells, and then treated them with RO8191 or TNF-α. In Huh-7 cells, NF-κB reporter gene was activated by TNF-α treatment, but not by RO8191 (Supplementary Fig. 3b). These results indicate that RO8191 specifically induces the IFN-relevant gene expressions.

Real-time RT-PCR analysis also revealed that RO8191 induced many ISGs similar to those expressed in IFN-α-treated cells (Fig. 2b and Supplementary Table 2), suggesting that the antiviral mechanism of RO8191 depends on ISG expression. In addition to HCV replicon cells, we tested the compound in several cancer cell lines and normal human primary hepatocytes (Hc cells). Real-time RT-PCR analysis showed that RO8191 induced ISG expression in cultured cell lines and human primary hepatocytes (Supplementary Table 3 and Supplementary Fig. 4). These results suggest that RO8191 induces an IFN signal, and that the application in clinical of RO8191 is not limited to suppressing HCV infection.

As mentioned earlier, type I IFNs phosphorylate JAK kinases and STAT proteins by inducing a heterodimerization of both IFNAR1 and IFNAR2, and the complexes thus formed transduce signals from IFN. Since RO8191 induces ISGs in a similar profile to IFN-α, we examined the phosphorylation of IFN signaling molecules. Immunoblotting analysis was performed to detect phosphorylated tyrosine (Tyr) and serine (Ser) residues of the STATs and JAK kinases using cell lysate that was treated with 50~5000 times the HCV replicon IC_{50}s of RO8191, IFN-α, IFN-β, and IFN-γ (type II IFN). The degree to which both RO8191 and IFN-β phosphorylated STAT1, STAT5, and STAT6 was similar, as shown in Fig. 2c, and the phosphorylation level of STAT2 by RO8191 was quite similar to that of IFN-α. Interestingly, STAT3 and JAK1 were more strongly phosphorylated by RO8191 than by IFN-α, -β, or -γ. On the other hand, Tyk2 was phosphorylated by type I IFNs, but not by IFN-γ or RO8191, indicating that Tyk2 is dispensable for RO8191 activity (Fig. 2c). Taken together, the phosphorylation profile of STAT proteins by RO8191 is generally similar to that of type I IFNs, and the phosphorylation profiles of STAT1–3, 5, 6, and JAK1 in HCV replicon cells treated with RO8191 or type I IFNs suggest a common mechanism that differs from the mechanism in cells treated with type II IFN.

In addition to imiquimod, an IFN inducer and a Toll-like receptor (TLR) 7 agonist[24], small-molecule ligands recognized by TLRs and RIG-I–like receptors are known to induce ISG expression by inducing IFN[25]. The chemical structure of RO8191 is similar to imiquimod so we examined whether RO8191 has a mechanism of activity like imiquimod. However, imiquimod did not affect HCV replicon cells (Supplementary Fig. 5a) and, moreover, did not stimulate

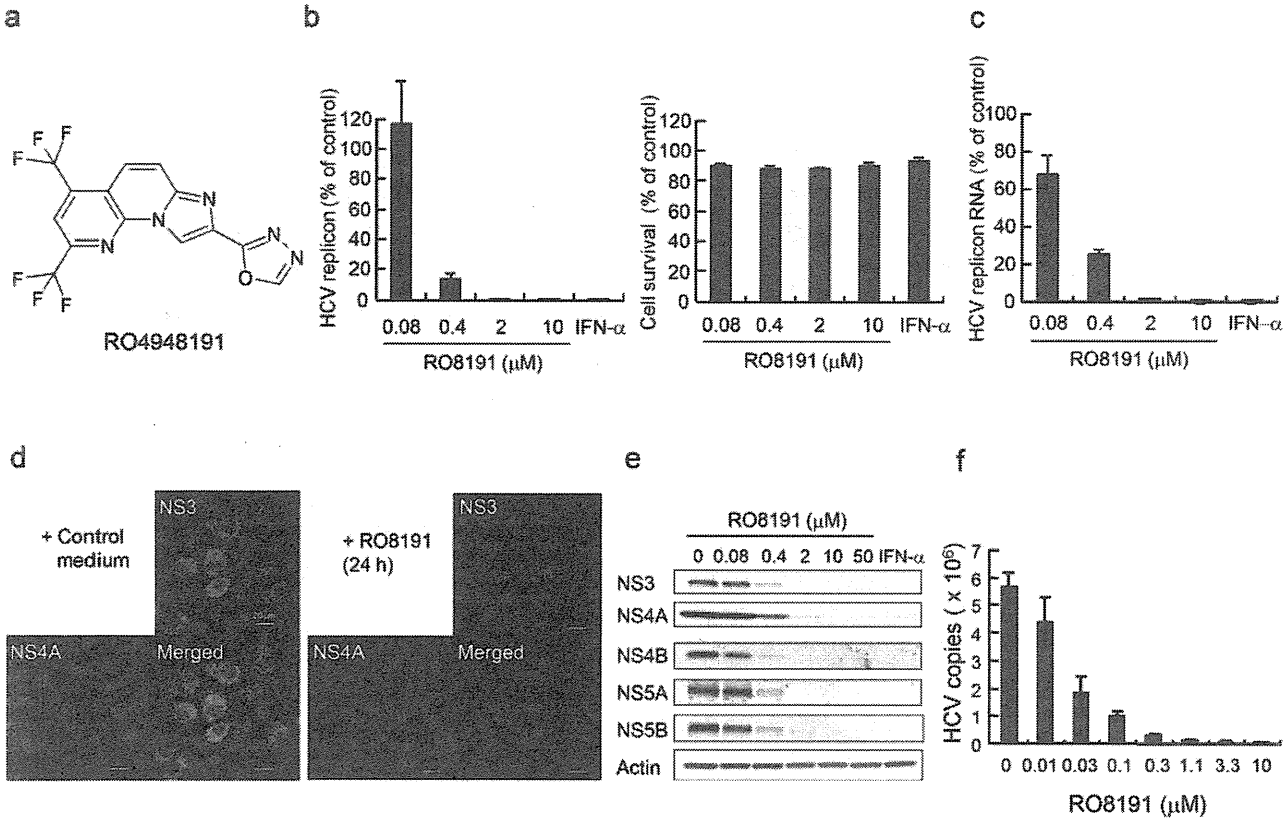

Figure 1 | Identification of a small molecule that inhibits HCV replication. (a) The chemical structure of RO8191. (b) After treatment with various concentrations of RO8191 or 100 IU/mL IFN-α for 72 h, HCV replication levels were examined using a luciferase assay (left graph), and cell viabilities were determined using a WST-8 assay (right graph). The mean values and their SDs were recorded for treated cells as a percentage of the values for untreated cells, and the values represent the means of 3 independent experiments. (c) Total RNA was extracted from HCV replicon cells cultured with the indicated concentration of RO8191 or 100 IU/mL IFN-α for 72 h; HCV RNA levels were analyzed using real-time RT-PCR. The mean values and their SDs were recorded for treated cells relative to the mRNA levels of β-actin, and are shown as a percentage of untreated cells. The values represent the means of 3 independent experiments. (d) HCV replicon cells were treated with control medium (left panels) or 10 μM RO8191 (right panels) for 24 h and immunostained with Hoechst 33452 (blue), anti-NS3 antibody (green), and anti-NS4A antibody (red). The results were then merged (yellow). (e) HCV replicon cells were treated with the indicated concentrations of RO8191 or 100 IU/mL IFN-α for 72 h. Whole cell lysates were immunoblotted with antibodies specific to the indicated HCV NS proteins. (f) After infection with the HCV JFH1 strain, Huh-7/K4 cells were treated with the indicated concentrations of RO8191 for 72 h. Total RNA was extracted, and the HCV RNA levels were analyzed using quantitative real-time RT-PCR.

STAT1 phosphorylation, whereas RO8191 caused prolonged STAT1 activation (for up to 8 h post-treatment; Supplementary Fig. 5b). Next, RO8191 is actually a small-molecule and we could not exclude the possibility that the antiviral activity might be induced through TLRs. To confirm that, we tested ISG induction using Tlr3, 4, 7 and 9 knockout (KO) mouse embryo fibroblasts (MEF)[24,26–28]. We treated the MEFs with RO8191 or murine IFN-αA for 8 h and both induced Oas1b mRNA in wild type and Tlr-KO MEFs (Supplementary Fig. 5c), demonstrating that RO8191 induces ISG expressions independently of TLRs. To exclude the possibility that RO8191 acts by inducing type I IFN, we examined its effects in Vero cells that lack the IFN gene locus[29,30]. Whereas imiquimod did not show IFN-like effects in Vero cells, RO8191 and IFN-α induced the ISRE activation (Supplementary Fig. 5d), indicating that RO8191 acts independently of the inducing IFN and is quite distinct from imiquimod.

RO8191 exerts antiviral activity dependent on IFNAR2/JAK1, but is independent of IFNAR1/Tyk2. IFNs require IFN receptor subunits for their activity, and we hypothesized that RO8191 uses the IFN receptor to exert anti-HCV activity. To determine the contributions of IFNAR1 and IFNAR2 toward the anti-HCV replicon activity of RO8191, we suppressed the expression of these receptors using specific siRNA and treated the cells with RO8191 or IFN-α. The knockdown efficiency was determined using RT-PCR in the HCV replicon cells transfected with each siRNA, as shown in Supplementary Fig. 6. As expected, a knockdown of each receptor subunit decreased the antiviral activity of IFN-α (Fig. 3a and b, Supplementary Fig. 7a and b). IFNAR2 knockdown attenuated the antiviral activity of RO8191 (Fig. 3b and Supplementary Fig. 7b) but, interestingly, IFNAR1 knockdown did not change the antiviral activity (Fig. 3a and Supplementary Fig. 7a), suggesting that RO8191 is independent of IFNAR1. To address whether IFN-α receptor contributes to RO8191 signaling, we evaluated RO8191 using Ifnar1-KO MEF cells[31]. We treated Ifnar1-KO MEFs with 50 μM RO8191 or 1,000 IU/mL of murine IFN-αA for 8 h and analyzed the expression of murine *Oas1b* mRNA using real-time RT-PCR. Murine IFN induced murine *Oas1b* mRNA only in wild type MEFs, not in Ifnar1-KO MEFs, although RO8191 induced *Oas1b* in both wild type and Ifnar1-KO MEFs (Supplementary Fig. 8). Therefore, RO8191 induces IFN-like activity even in Ifnar1-KO MEFs.

Since IFNAR2 knockdown reduced RO8191 activity, we focused on and analyzed the IFNAR2 function using RO8191. First, U5A cells, which do not respond to IFN-α because of the lack of

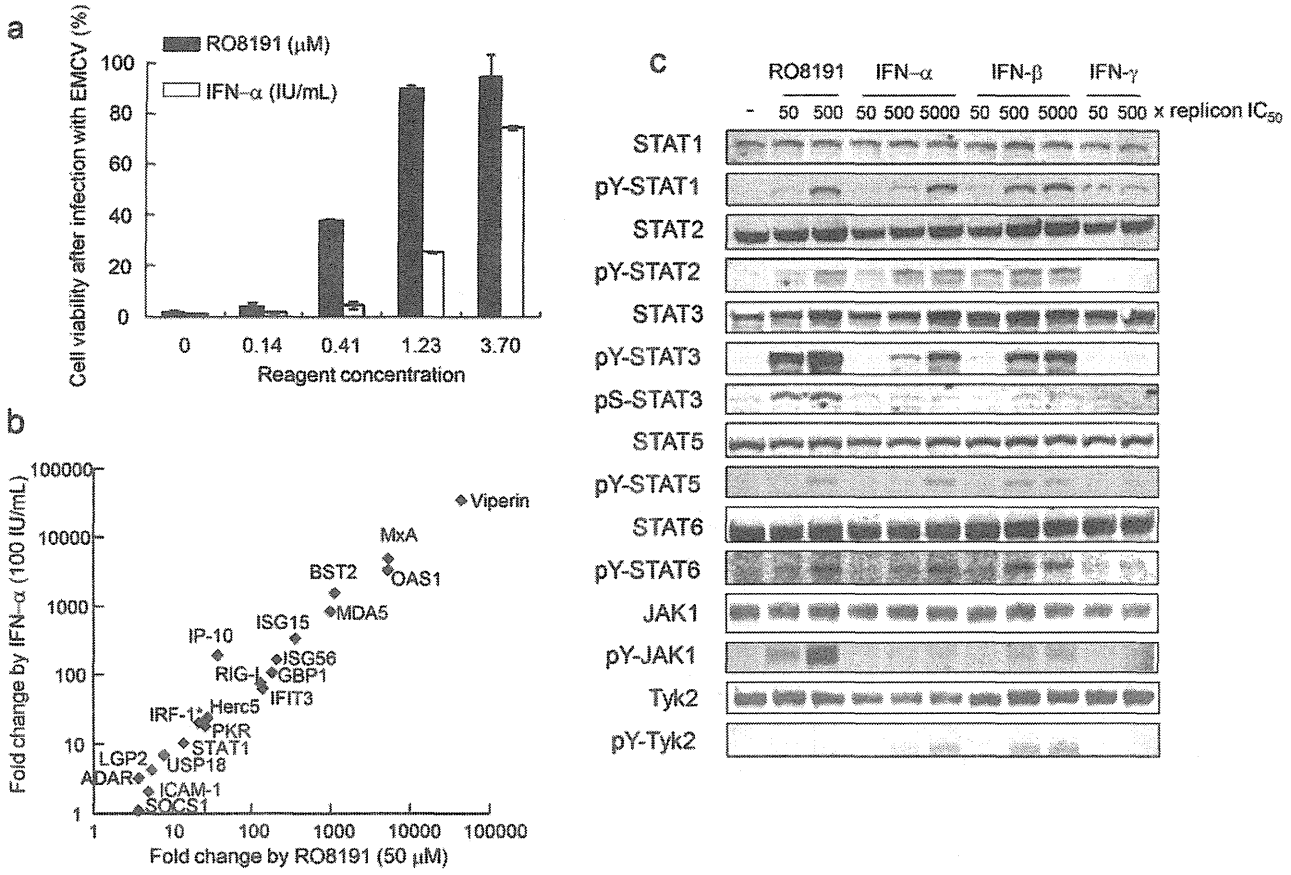

Figure 2 | RO8191 activates JAK/STAT and induces IFN-like signals. (a) The cytopathic effect of EMCV infection was inhibited by the indicated concentrations of RO8191 or IFN-α. Viable cells were stained with crystal violet. The data shown are the mean values and SDs based on experiments performed in quadruplicate. (b) ISG expression levels were measured using real-time RT-PCR. Total RNA was extracted from HCV replicon cells cultured in the presence of 50 μM RO8191 or 100 IU/mL IFN-α for 2 or 8 h and known ISGs were analyzed. Asterisk indicates 2-h treatment with agents. The values shown are the mean fold change induction compared to the mRNA level of human *β-actin* and the fold change induction compared to untreated cells. (c) HCV replicon cells were treated with various concentrations of the indicated agents for 15 min. Total lysates were immunoblotted with antibodies to STATs or JAK kinases. The HCV replicon IC_{50} of IFN-α was 0.4 IU/mL, that of IFN-β was 3 IU/mL, and that of IFN-γ was 0.3 ng/mL.

IFNAR2 expression[32], were treated with RO8191. Although RO8191 and IFN-α did not induce *OAS1* expression in the U5A cells, IFNAR2-overexpressing U5A cells were successfully complemented, and this conferred susceptibility to both RO8191 and IFN-α (Fig. 3c and d). RO8191 also induced the *OAS1* gene in HT1080 and 2fTGH cells, the parental cell lines of U5A cells (Supplementary Table 3, lowest and second lowest rows). Second, to elucidate whether RO8191 directly interacts with IFNAR2, we obtained a recombinant IFNAR2 extracellular domain (ECD) protein (N-terminal half of the protein, amino acids from Ile27- Lys243). The protein was subjected to surface plasmon resonance (SPR) spectroscopy using a Biacore system to directly evaluate the binding activity of the recombinant protein with its possible ligands, RO8191 and IFN-α. The IFNAR2 ECD protein was fixed on the surface of the CM7 sensor chip by amine coupling, and PEG-IFN-α2a and RO8191 were injected as analytes. We comparatively analyzed 0.31 and 0.63 μM of RO8191, and both concentrations showed similar binding affinities of 480.5 and 484.5 nM, respectively (Fig. 3e), whereas a chemically derivatized compound of RO8191 that cannot inhibit HCV replication did not bind to IFNAR2 ECD (data not shown). The SPR results were consistent with 1:1 binding and showed an interaction between RO8191 and the IFNAR2 ECD protein in a dose-dependent manner, indicating that the compound and IFNAR2 may directly interact on the cell surface. In addition to the anti-replicon activity, the phosphorylation of STAT1 by RO8191 was also repressed by IFNAR2 knockdown (Fig. 3g), but the knockdown of IFNAR1 did not inhibit the STAT1 phosphorylation (Fig. 3f), indicating that RO8191 requires IFNAR2 but not IFNAR1 to achieve activity. Similarly, the knockdown of JAK1 attenuated the activity of RO8191 and IFN-α (Fig. 4a and Supplementary Fig. 9a), while, in contrast, Tyk2 and JAK2 were not required for RO8191 activity (Fig. 4b, Supplementary Fig. 9b and c). The phosphorylation of STAT1 by RO8191 was also inhibited by a knockdown of JAK1 (Supplementary Fig. 10a), but not by a knockdown of Tyk2 (Supplementary Fig. 10b), indicating JAK1 essentiality for the antiviral activity of RO8191. To confirm Tyk2-independency, we used U1A (Tyk2-deficient) cells and the parental cell, 2fTGH[33], and treated them with 50 μM RO8191 or 100 IU/mL IFN-α for 8 h to analyze the expression of *OAS1*. As expected from previous reports[34], IFN-α induced the *OAS1* expression only in 2fTGH cells but not in U1A cells; however, RO8191 induced the expression in both 2fTGH and U1A cells significantly (Supplementary Fig. 11). Thus, RO8191 activates ISGs in a JAK1-dependent and Tyk2-independent manner; on the other hand, IFN-α depends on both factors. Next, we conducted a knockdown of the transcription factors related to type I IFNs activity, STAT1, STAT2 and IRF-9, to clarify whether RO8191 required these factors for antiviral activity. As expected, STAT1-siRNAs partially blocked IFN-γ activity (Supplementary Fig. 9d),

Table 1 | ISG expression in the livers of RO8191 treated mice. ISG expression levels were measured using real-time RT-PCR. Values are listed relative to the mRNA levels of rodent *Gapdh* and represent the mean fold change induction compared to vehicle-administered mice. Twenty-four hours after oral administration of 30 mg/kg RO8191 or vehicle (including 10% dimethyl sulfoxide and 10% Cremophor) to mice, total RNA was extracted from the mouse livers, and the mRNA levels of murine ISGs were measured using real-time RT-PCR. The data shown are the means and SDs of 4 mice per group. The data were statistically analyzed using Student's *t*-test, and differences were considered significant at p values < 0.05

Gene	Entrez ID	Fold change ± SD			p-value
murine Oas1	NM_001083925	3.0	±	0.72	0.003
murine Mx1	NM_010846	2.1	±	0.15	0.0003
murine Pkr	NM_011163	1.4	±	0.21	0.009
murine Cxcl10	NM_021274	1.7	±	0.63	0.097
murine Ifit3	NM_010501	2.5	±	0.48	0.001
murine Isg15	NM_015783	2.3	±	0.41	0.002
murine Mda5	NM_027835	1.6	±	0.22	0.003
murine Rig-i	NM_172689	2.1	±	0.16	0.00003
murine Socs1	NM_009896	2.6	±	1.04	0.057
murine Stat1	NM_009283	1.8	±	0.21	0.001
murine Usp18	NM_011909	2.6	±	0.69	0.017

which is mediated by STAT1 homodimers[35]. STAT1 was significantly phosphorylated by both RO8191 and IFN-α (Fig. 2c); however, the STAT1 knockdown affected neither RO8191 nor IFN-α activity (Fig. 4c and Supplementary Fig. 9d). We also analyzed the impact of STAT1 knockdown on *OAS1* induction by RO8191, and found *OAS1* induction by RO8191 was inhibited (Supplementary Fig. 12). STAT2 and IRF9 knockdown attenuated the inhibitory activity of both RO8191 and IFN-α (Fig. 4d and e and Supplementary Fig. 9e and f). In summary, RO8191 only binds to IFNAR2 and activates JAK1, STATs, and IRF9, thereby exhibiting type I IFN-like activity (Fig. 4f).

RO8191, an IFNAR2 agonist, stimulates IFN signals in mice. To evaluate whether RO8191 could be a clinical lead for drug development, we studied the effects of RO8191 on IFN signaling in mice. The compound or vehicle was orally administered to mice and, 24 h after treatment, the liver was removed and examined. The antiviral genes *Oas1b*, *Mx1*, and *Pkr* were significantly induced in the livers of mice treated with RO8191 (Table 1). As expected, gene homologs that were induced in the livers of HCV patients treated with PEG-IFN-α2b[36] were also induced in mouse liver (*Ifit3*, *Isg15*, *Mda5*, *Rig-I*, *Socs1* and *Stat1*; Table 1). In addition, genes that had previously been reported to be induced by IFN-β in mouse liver[37] were also induced in the livers of RO8191-treated mice (*Cxcl10*, *Ifit3*, *Isg15*, *Socs1* and *Usp18*; Table 1,). We also measured inflammatory cytokine and chemokine expressions, and RO8191 did not significantly induce the expression of these genes (Supplementary Table 4). To evaluate anti-HCV activity of RO8191 *in vivo*, RO8191 was orally administered to HCV-infected humanized liver mice[38]. The results of this humanized liver mice study showed that RO8191 reduced HCV titer *in vivo* (Supplementary Fig. 13). These data show that RO8191 stimulates IFN signaling and is an orally available agent in mice.

Discussion

In this study, we identified a small-molecule IFN receptor agonist, RO8191, by quantitative HTS of a chemical library. This compound showed antiviral activity against both HCV and EMCV, suggesting a broad spectrum of target viruses. To learn more about the possible mechanism of action of IFN signal induction by RO8191, we investigated IFN-induced signaling and ISG induction by the small-molecule compound *in vitro* and *in vivo*. A comparison of microarray expression profiles in HCV replicon cells stimulated by IFN-α or RO8191 indicates that the IFN signal was induced not only by IFNs, but also by the small-molecule compound (Fig. 2b and Supplementary Fig. 2). Thus, this compound is an IFN-α-like small molecule, but the mechanism of the RO8191 antiviral activity remained unknown. Therefore, we examined the JAK/STAT activation pathway, which includes key players in the IFN signaling cascade.

Like type I IFNs, RO8191 significantly phosphorylates and activates STATs, in particular, STAT1 and STAT2 (Fig. 2c). Intriguingly, in HCV replicon cells, STAT1 expression knockdown did not affect the antiviral activity of RO8191 or IFN-α, although IFN-γ activity was inhibited (Fig. 4c). These data suggest that, in addition to inducing similar gene expression, RO8191 and IFN-α exhibit similar STAT phosphorylation profiles. Although RO8191- and IFN-α-mediated antiviral activity remained constant when STAT1 expression was reduced, this could be because IFN-α signaling in HuH-7 cells requires minimal amounts of STAT1 protein and STAT1 expression was not reduced below such a critical threshold by siRNA in our system. In contrast, the inhibitory activity of RO8191 was attenuated to the same extent as that of IFN-α when the expression of other components of ISGF3 (STAT2 and IRF-9) were reduced by siRNA (Fig. 4d and e). Incidentally, STAT1 siRNA did not attenuate RO8191 or IFN activity in EMCV-infected A549 cells (supplementary Fig.14), which supports the notion that STAT2 is an essential component of type I IFN signaling[39]. Type I IFN stimulates the formation of other STAT-containing complexes, including STAT1:STAT1, STAT3:STAT3 and STAT5:STAT5 homodimers, as well as STAT1:STAT3 and STAT2:STAT6 heterodimers[40–42]. Like IFN, RO8191 induced the phosphorylation of STAT1 and STAT2, which function as a gateway to the type I IFN signal cascade, and stimulated the phosphorylation of STAT3, 5 and 6. Another possible cause for the fact that STAT1 knockdown did not show any effect on RO8191 inhibition could be compensation by these IFN signaling-stimulated STAT complexes. This finding matches the recent report by Perry *et al.* on the STAT dependency of IFN activity against Dengue virus, that belongs to flavivirus[43]. They showed that STAT2 mediates IFN antiviral signals even in STAT1 KO cells and they discussed the possibility that other STAT family proteins would compensate for STAT1 deficiency. In summary, with regards to the activation of transcription factors and ISG expression, RO8191 and IFN-α mediate the same pathway.

IFNs activate JAK kinases via IFN receptors to induce STAT phosphorylation. RO8191 robustly phosphorylated JAK1 (Fig. 2c) in comparison with IFN-α or -β and therefore we focused on IFNAR2 (a JAK1-binding subunit of the type I IFN receptor). As with IFN-α, the activity of RO8191 was inhibited by IFNAR2 knockdown (Fig. 3b). The suggestion that IFNAR2 is an essential molecule for RO8191-induced signal transduction is supported by the fact that an IFNAR2-deficient cell line, U5A, did not respond to RO8191. Furthermore, after IFNAR2 expression had been complemented in the U5A cells, ISG induction by both RO8191 and IFN-α recovered (Fig. 3c and d). The mechanism was directly explained by SPR spectroscopy, which showed an interaction between RO8191 and the IFNAR2 ECD (Fig. 3e). RO8191 strikingly phosphorylates the IFNAR2-associated kinase JAK1, when compared to other IFN-treated cell lysates (Fig. 2c). JAK1 siRNA expression inhibited RO8191 activity (Fig. 4a), indicating that JAK1 is also an essential molecule for RO8191 activity. Interestingly, RO8191 activity remains static when IFNAR1 expression is knocked down, unlike IFN-α activity (Fig. 3a). The IFNAR1-binding-kinase Tyk2 is not required for RO8191 activity (Fig. 4b) and Tyk2 was not phosphorylated (Fig. 2c) by RO8191. Also, RO8191 induced its signal even in the Ifnar1 KO MEF and the Tyk2-deficient cell line (Supplementary Fig.

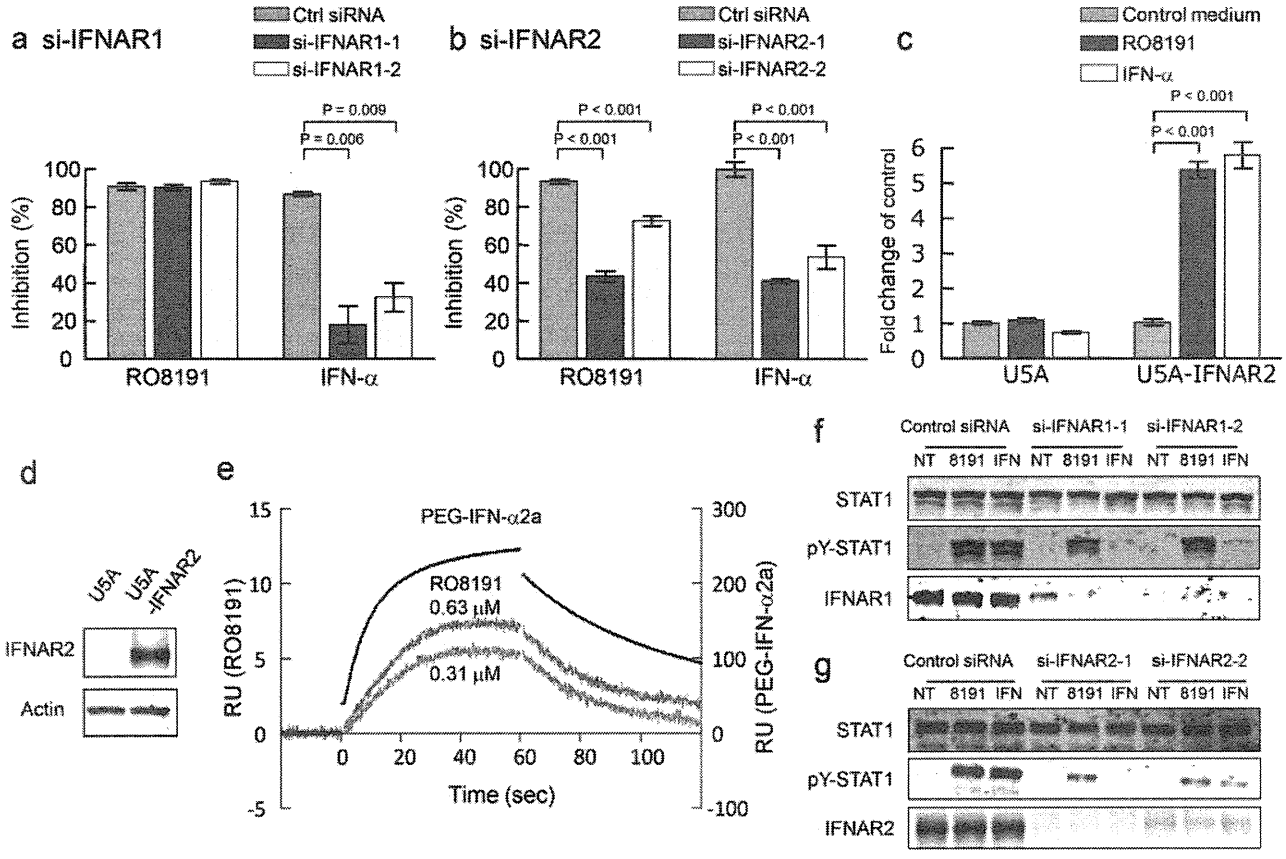

Figure 3 | RO8191 requires and binds IFNAR2. (a, b) The anti-HCV replicon activity of RO8191 was attenuated by knockdown of IFNAR2 (b), but not IFNAR1 (a). Inhibition of HCV replicon replication by each agent is shown (the mean and SD from 3 experiments). The HCV replicon cells were transfected with 50 nM of the indicated siRNAs (blue, red, and yellow bars). Forty-eight hours after transfection, the HCV replicon cells were treated with 1.5 μM RO8191 or 3 IU/mL IFN-α for 24 h. Twenty-four hours after treatment with each agent, the replication levels of HCV RNA were analyzed using a luciferase assay. (c, d) U5A cells that lack IFNAR2 were transfected with either an empty vector or a vector expressing the *IFNAR2* gene. (c) Forty-eight hours after transfection, the cells were treated with 50 μM RO8191 (red bars) or 100 IU/mL IFN-α (yellow bars). After an additional 8 h of incubation, total RNA was extracted from the U5A cells, and the *OAS1* mRNA level was measured using real-time RT-PCR. The values shown are relative to the mRNA level of human *β-actin*. (d) Forty-eight hours after transfection, the cells were lysed, and the whole cell lysates were immunoblotted with the indicated antibodies. (e) Real-time kinetic SPR analysis of the binding of RO8191 to the IFNAR2 ECD (red and blue lines). The results are consistent with 1:1 binding. PEG-IFN-α2a was also injected as a positive interacting control for IFNAR2 (black line, K_D: 30 nM). (f, g) The phosphorylation of STAT1 was attenuated by a knockdown of IFNAR2 (g) but not IFNAR1 (f). The HCV replicon cells were transfected with the indicated siRNAs (10 nM). Forty-eight hours after transfection, the cells were treated for 15 min with 10 μM RO8191 or 200 IU/mL IFN-α. The total lysates were subjected to western blot analysis to analyze the phosphorylated and total protein levels of STAT1. The data were statistically analyzed using Student's *t*-test.

8 and 11). IFN-α induces a signal via IFNAR1/Tyk2 and IFNAR2/JAK1 although RO8191 and IFN-α induce common ISGs (Fig. 2b and Supplementary Fig. 2), RO8191 activity was dependent only on IFNAR2.

We therefore propose a novel model of the induction of IFN-like signal transduction by this small molecule (Fig. 4f). So far, the IFNAR2 homodimer has been suggested to play various roles in IFN signal transduction[34,44,45], and RO8191 would induce the ISG expression via such IFNAR2 homodimer. For type I IFN, both IFNAR1 and IFNAR2 cooperate and induce phosphorylation of STATs via JAK1 and Tyk2. Conversely, for RO8191, IFNAR2 alone, as a homodimer, activates JAK1 phosphorylation and subsequent STATs activation. Experiments using siRNA and deficient cells have also shown that IFNAR1 and Tyk2 were not required to induce antiviral activity in the RO8191 compound pathway. These findings suggest a novel aspect of the IFN signaling pathway that may contribute to the understanding of other molecular signaling in IFN pathways.

RO8191 is a small molecule whose oral administration is feasible and effective in a murine model (Table 1 and Supplementary Fig. 13). In the chimeric mice study, the anti-HCV effect of RO8191 and PEG-IFN was similar in that they both showed strong activity at day 1 after treatment with subsequent weak suppression of HCV replication possibly due to the immunodeficiency of chimeric mice. Further development of RO8191 by using rational chemical modifications is therefore required to produce more potent molecules for testing as an antiviral molecule which will substitute current recombinant IFN. Although RO8191 has the potential to cause IFN-like adverse effects, further development of the small-molecule agonist offers the advantages of inexpensive production cost, convenient oral administration, dose-control to reduce some adverse effects, and potentially increased activity versus current recombinant IFNs.

Whereas oral NS3 protease inhibitors in monotherapy development yield resistant viruses[46,47], these protease inhibitors show a significantly high rate of SVR when combined with PEG-IFN[10,11] and a NS5B polymerase inhibitor also shows additive efficacy in combination with PEG-IFN[48]. In addition to the results of the *in vivo* study, we found that RO8191 induced ISGs at a level similar to IFN-α in human primary hepatocytes (Supplementary Fig. 4); we therefore expect that RO8191 will show IFN-like activity in clinical use. As an

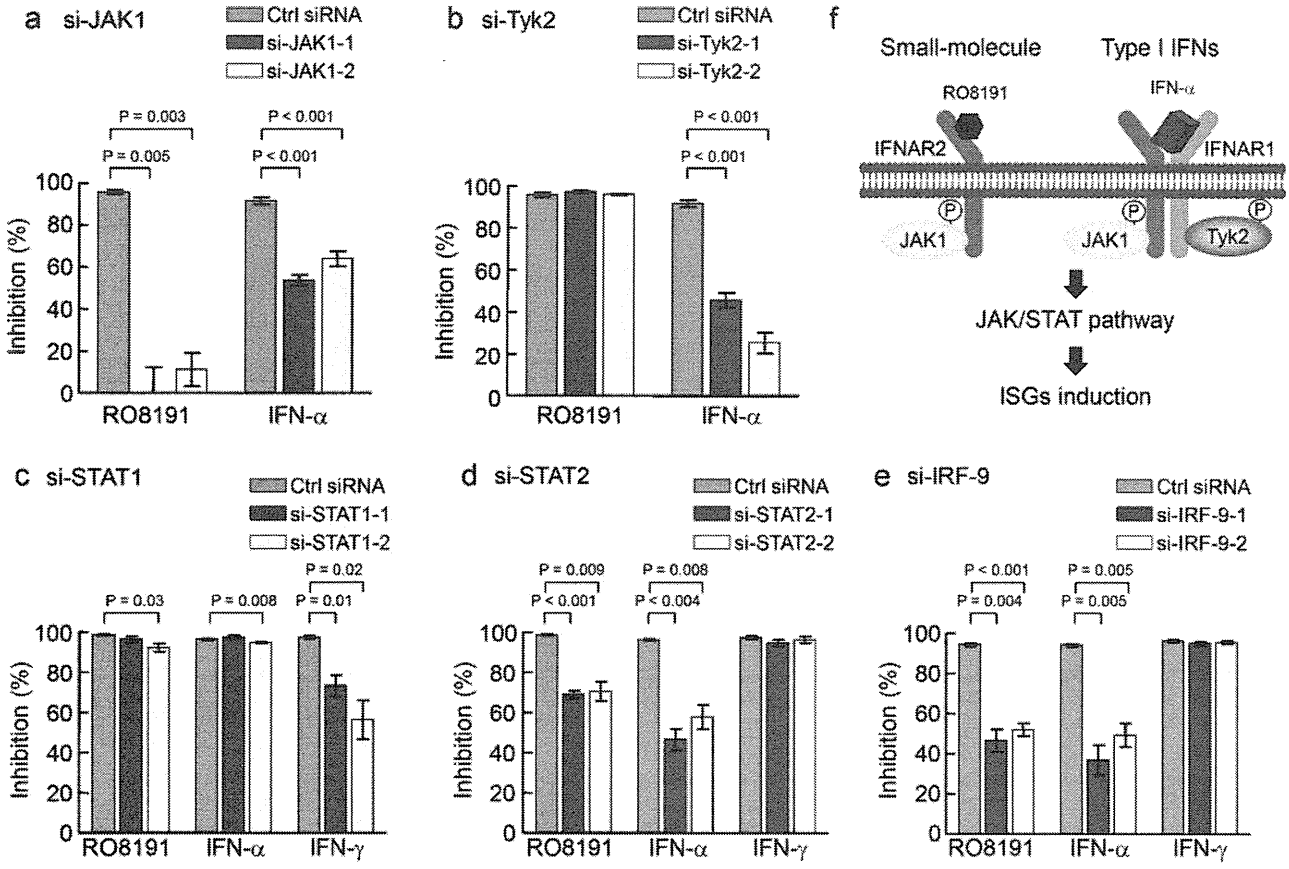

Figure 4 | RO8191 activates a novel IFN-like pathway. (a–e) The inhibition of HCV replicon replications by each agent is shown (mean and SD). The HCV replicon cells were transfected with 50 nM of the indicated siRNAs (blue, red, and yellow bars). (a, b) The anti-HCV replicon activity of RO8191 was reduced by knockdown of JAK1 (a) but not Tyk2 (b). Forty-eight hours after transfection, the HCV replicon cells were treated with 1.5 μM RO8191 or 3 IU/mL IFN-α. Twenty-four hours after treatment with each agent, the replication levels of HCV RNA were analyzed using a luciferase assay. (c–e) The anti-HCV replicon activity of RO8191 was reduced by knockdowns of STAT2 (d) and IRF9 (e), but not STAT1 (c). Forty-eight hours after transfection, the HCV replicon cells were treated with 1.5 μM RO8191, 3 IU/mL IFN-α, or 50 ng/mL IFN-γ. Twenty-four hours after treatment, the replication levels of HCV RNA were analyzed using a luciferase assay. (f) A schematic showing the pathways of RO8191 and IFN-α. The data were statistically analyzed using Student's *t*-test, and differences were considered significant at p values < 0.05.

alternative strategy to protease/polymerase inhibitors with PEG-IFN, the combined use of these direct-acting antiviral agents with RO8191 in a new oral regimen may help overcome some of the delivery problems associated with current IFNs. SVR rates of individuals infected with HCV genotype 1 have increased from 5-20% with IFN monotherapy and up to 50% with a combination of IFN and ribavirin. However, the refractory patients in this therapy constitute an unmet medical need. Thus, the development of a novel IFN receptor agonist, used alone or in combination with direct-acting antiviral drugs, will add a new milestone to the treatment of chronic hepatitis C. In addition to HCV infection, type I IFNs have been approved for the treatment of multiple clinical conditions, including hairy cell leukemia, malignant melanoma, AIDS-related Kaposi's sarcoma, multiple sclerosis, and chronic hepatitis B[49]. Thus, R08191 shows strong potential as a lead compound for IFN substitutes.

Methods

Cell culture, mice, and reagents. The #Huh7/3-1 cell line, which expresses HCV replicons, was a kind gift from F. Hoffmann-La Roche. The cells were cultured in 0.5 mg/mL G418-containing Dulbecco's modified Eagle's medium (DMEM, GIBCO) supplemented with 10% fetal bovine serum (FBS, HyClone). The replicon construct was derived from pFK-I377neo/NS3-3′/WT, as previously reported[19]. Hc cells (DS Pharma Biomedical) were cultured in CSC Complete Defined Serum-Free Medium (Cell Systems Corporation) supplemented with SF4ZR-500-D Rocket Fuel. Tlr KO MEFs were purchased from OrientalBioService, Inc. Ifnar1 KO MEF was kindly gifted by Prof. Takaoka. 2fTGH, and U1A and U5A cells were kindly gifted by Prof. Stark. Culture conditions for the other cell lines are shown in Supplementary Table 5. Six-week-old C57BL/6J mice were obtained from Charles River Laboratories. Chimeric mice harboring a functional human liver cell xenograft were purchased from PhoenixBio. The protocol was reviewed by the Institutional Animal Care and Use Committee of Chugai Pharmaceutical Co., Ltd. and all mouse experiments were performed in accordance with the Guidelines for the Accommodation and Care of Laboratory Animals promulgated in Chugai Pharmaceutical Co., Ltd. Recombinant human IFN-α2a was a kind gift from F. Hoffmann-La Roche. Recombinant murine IFN-αA and human IFN-β1a were purchased from PBL Interferon Source. Recombinant TNF-α and IFN-γ were purchased from R&D Systems. Imiquimod was purchased from LKT Laboratories. JAK inhibitor I was purchased from Merck.

Luciferase assay. Luciferase activity was quantified using the Steady-Glo Luciferase assay system (Promega) and the EnVision 2013 Multilabel Reader (PerkinElmer).

WST-8 assay. The viability of drug-treated Huh-7 cells was determined using a WST-8 cell counting kit (Dojin Laboratories).

Real-time RT-PCR. Total RNA was extracted using Rneasy (Qiagen), and cDNA was synthesized using a Transcriptor First Strand cDNA Synthesis Kit (Roche Applied Science). Gene expression was measured using the LightCycler 480 System and LightCycler 480 Probes Master (Roche Applied Science). The amplification used 50 cycles of: 95°C for 5 min, 95°C for 10 s, and 60°C for 30 s. Human β-actin or rodent glyceraldehyde 3-phosphate dehydrogenase (GAPDH; Applied Biosystems) expression was used as the endogenous reference for each sample. Primers and TaqMan probes for genes were designed using the Universal Probe Library Assay Design Center (Roche Applied Science; Supplementary Table 6). The probes used were from the Roche Universal Probe Library (Roche Applied Science). The samples

were run in triplicate for each target gene, and each reference gene was used as an internal control.

Western blotting and immunostaining. Cells were lysed in CelLytic M Cell Lysis Reagent (Sigma-Aldrich) containing Protease Inhibitor Cocktail (Sigma-Aldrich) and PhosSTOP (Roche Applied Science). Rabbit polyclonal antibodies against STAT1, STAT3, STAT6, pY701-STAT1, pY690-STAT2, pY705-STAT3, pS727-STAT3, pY694-STAT5, pY641-STAT6, pY1022/1023-JAK1, and pY1054/1055-Tyk2 were purchased from Cell Signaling Technology. Rabbit polyclonal antibodies against actin, STAT2 and STAT5 were purchased from Santa Cruz Biotechnology. Anti-Tyk2 rabbit polyclonal antibody was purchased from Upstate. Anti-IFNAR1 mouse monoclonal (MAB245) and anti-IFNAR2 sheep polyclonal antibodies were purchased from R&D Systems. Anti-NS3, anti-NS5A, and anti-NS5B rabbit polyclonal antibodies were a kind gift from F. Hoffmann-La Roche. Anti-NS4A and anti-NS4B mouse monoclonal antibodies were a kind gift from the Tokyo Metropolitan Institute of Medical Science. Proteins were detected using the Odyssey Infrared Imaging System (LI-COR). For immunostaining analysis, the cells were fixed on a 35-mm glass-based dish (Iwaki) with 4% paraformaldehyde, blocked using 5% fetal bovine serum in phosphate-buffered saline, and then incubated with anti-NS3 and anti-NS4A antibodies. The cells were then washed and incubated with Alexa488-labeled anti-rabbit IgG and Alexa568-labeled anti-mouse IgG (Molecular Probes) and analyzed using confocal laser microscopy.

JFH-1 antiviral assay. A cured K4 cell line derived from HuH-7 HCV replicon cells was maintained in DMEM supplemented with 10% fetal calf serum (FCS), high-glucose nonessential amino acids, and HEPES (Invitrogen). The JFH-1/K4 cell line, which was persistently infected with the HCV JFH-1 strain, was maintained under the same conditions as the cured K4 cell line. For the anti-HCV assay of JFH-1/K4 cells persistently infected with the JFH-1 strain, JFH-1/K4 cells were seeded in a 24-well tissue culture plate containing DMEM supplemented with 10% FCS, high-glucose nonessential amino acids, and HEPES (Invitrogen). After overnight incubation, serial dilutions of reagent in growth medium were added. After 72 h, total RNA was purified from the JFH-1/K4 cells using Isogene (Nippon Gene). HCV-RNA was quantified by real-time PCR as previously reported[50].

EMCV cytopathic effect assay. This assay was performed on A549 cells seeded in a 96-well tissue culture plate containing DMEM supplemented with 10% FBS. After overnight incubation, the indicated concentrations of each reagent were added to the growth medium. After 12 h, 100 $TCID_{50}$/mL EMCV was added, and after another 48 h, viable cells were stained with 0.5% crystal violet. RNAi experiment using EMCV was also performed on A549 cells seeded in a 96-well tissue culture plate containing DMEM supplemented with 10% FBS. We transfected STAT1- or STAT2-siRNA to A549 cells, and after 72 h we infected EMCV to the cells and treated them with 1 μM RO8191 or 2 IU/mL IFN. After additional 48 h incubation, we evaluated the cell viability by staining with crystal violet.

GeneChip and data analysis. Total RNA was extracted from 10^7 HCV replicon cells cultured for 8 h in the presence of 2 μM RO8191 or 4 IU/mL IFN-α with TRIzol Reagent (Invitrogen). Reverse transcription, RNA labeling (5 μg of total RNA), hybridization to Human Genome U133 Plus 2.0 Arrays (Affymetrix), and scanning were performed according to the manufacturer's instructions (Affymetrix, http://www.affymetrix.com). GC-RMA (GeneChip Robust Microarray Analysis) algorithms were used to generate scaled gene expression values. The fold change compared to untreated cells was calculated, and probe sets were selected for genes that were at least 2.0-fold upregulated in RO8191- and IFN-α-treated cells relative to the control cells.

RNA interference. For all double-stranded RNAs, ON-TARGET Plus siRNA reagents (Dharmacon) were used (Supplementary Table 7). The siRNAs were transiently transfected using Lipofectamine RNAiMAX Transfection reagent (Invitrogen) according to the manufacturer's protocols for reverse transfection.

Plasmids and transfection. ISRE and NF-κB reporter gene were purchased from Clontech. *IFNAR2* was cloned into a pCOS2 vector[51] harboring the EF1α promoter. Plasmids were transfected using FuGENE HD (Roche Applied Science) according to the manufacturer's instructions.

SPR measurements. SPR binding studies were performed using a Biacore T100. Recombinant IFNAR2 ECD protein was purchased from R&D Systems. The protein (1 mg/mL) was diluted 1:20 with 10 mM sodium acetate buffer (pH 5.0) and mixed with 2 μM RO8191 for stabilization of the binding site. The mixture was immobilized on a Series S sensor chip CM7 using amine coupling. RO8191 and PEG-IFN-α2a (Chugai Pharmaceutical) were injected onto the sensor chip at a flow rate of 0.03 mL/min. Response curves were generated by subtraction of the background signal generated simultaneously on a control flow cell. Kinetic parameters were obtained by global fitting of the sensorgrams to a 1:1 model using Biacore T100 Evaluation Software, version 2.0.1.

Humanized liver mice study. The chimeric mice were generated by transplanting human primary hepatocytes into severe combined immunodeficient (SCID) mice carrying the urokinase plasminogen activator transgene controlled by an albumin promoter[38]. The chimeric mice used in this study were applied from Inoue *et al.*[52], and had a high substitution rate of human hepatocytes. Six weeks after hepatocyte transplantation, patient serum containing 10^6 copies of HCV genotype 1b was intravenously injected into each mouse. HCV titer reached approximately 10^8 copies/mL and was stable after 4 weeks of HCV injection and persistently infected for 12 weeks. Here, we used mice after 5 weeks post infection and tested for 2 weeks. The mice were treated for 14 days with RO8191 30 mg/kg/day orally or PEG-IFN-α2a 30 μg/kg subcutaneously twice weekly. HCV RNA in serum was extracted using the acid guanidinium-phenol-chloroform method. Quantification of HCV RNA was performed using real-time RT-PCR based on TaqMan chemistry, as described[50]. HCV inoculations, drug administration, blood collection, and killing were performed under ether anesthesia. Blood samples were taken from the orbital vein and sera were immediately isolated. The protocols for animal experiments were approved by the local ethics committee. The animals received humane care according to NIH guidelines. Patients gave written informed consent before sampling.

1. Lavanchy, D. The global burden of hepatitis. *Liver Int.* **29**, 74–81 (2009).
2. Ghany, M. G., Strader, D. B., Thomas, D. L. & Seeff, L. B. Diagnosis, management, and treatment of hepatitis C: an update. *Hepatology.* **49**, 1335–74 (2009).
3. Zeuzem, S. Interferon-based therapy for chronic hepatitis C: current and future perspectives. *Nat Clin Pract Gastroenterol Hepatol.* **5**, 610–622 (2008).
4. Ge, D. *et al.* Genetic variation in IL28B predicts hepatitis C treatment-induced viral clearance. *Nature.* **461**, 399–401 (2009).
5. Suppiah, V. *et al.* IL28B is associated with response to chronic hepatitis C interferon-alpha and ribavirin therapy. *Nat Genet.* **41**, 1100–4 (2009).
6. Tanaka, Y. *et al.* Genome-wide association of IL28B with response to pegylated interferon-alpha and ribavirin therapy for chronic hepatitis C. *Nat Genet.***41**, 1105–9 (2009).
7. Thomas, D. L. *et al.* Genetic variation in IL28B and spontaneous clearance of hepatitis C virus. *Nature.* **461**, 798–801 (2009).
8. Czepiel, J., Czepiel, J., Biesiada, G. & Mach, T. Viral hepatitis C. *Pol Arch Med Wewn.* **118**, 734–740 (2008).
9. Webster, D. P., Klenerman, P., Collier, J. & Jeffery, K. J. Development of novel treatments for hepatitis C. *Lancet Infect Dis.* **9**, 108–117 (2009).
10. Jacobson, I. M. *et al.* Telaprevir for previously untreated chronic hepatitis C virus infection. *N Engl J Med.* **364**, 2405–16 (2011).
11. Poordad, F. *et al.* Boceprevir for untreated chronic HCV genotype 1 infection. *N Engl J Med.* **364**, 1195–206 (2011).
12. Kwong, A. D., McNair, L., Jacobson, I. & George, S. Recent progress in the development of selected hepatitis C virus NS3.4A protease and NS5B polymerase inhibitors. *Curr Opin Pharmacol.* **8**, 522–531 (2008).
13. Stark, G. R. *et al.* How cells respond to interferons. *Annu Rev Biochem.* **67**, 227–264 (1998).
14. de Veer, M. J. *et al.* Functional classification of interferon-stimulated genes identified using microarrays. *J Leukoc Biol.* **69**, 912–20 (2001).
15. Pestka, S., Langer, J. A., Zoon, K. C. & Samuel, C. E. Interferons and their actions. *Annu Rev Biochem.* **56**, 727–777 (1987).
16. Uze, G., Lutfalla, G. & Gresser, I. Genetic transfer of a functional human interferon alpha receptor into mouse cells: cloning and expression of its cDNA. *Cell.* **60**, 225–234 (1990).
17. Novick, D., Cohen, B. & Rubinstein, M. The human interferon alpha/beta receptor: characterization and molecular cloning. *Cell.* **77**, 391–400 (1994).
18. Lohmann, V. *et al.* Replication of subgenomic hepatitis C virus RNAs in a hepatoma cell line. *Science.* **285**, 110–113 (1999).
19. Sakamoto, H. *et al.* Host sphingolipid biosynthesis as a target for hepatitis C virus therapy. *Nat Chem Biol.* **1**, 333–337 (2005).
20. Wakita, T. *et al.* Production of infectious hepatitis C virus in tissue culture from a cloned viral genome. *Nat Med.* **11**, 791–796 (2005).
21. Kneteman, N. M. *et al.* Anti-HCV therapies in chimeric scid-Alb/uPA mice parallel outcomes in human clinical application. *Hepatology.* **43**, 1346–1353 (2006).
22. Dash, S. *et al.* Interferons alpha, beta, gamma each inhibit hepatitis C virus replication at the level of internal ribosome entry site-mediated translation. *Liver Int.* **25**, 580–594 (2005).
23. Der, S. D., Zhou, A., Williams, B. R. & Silverman, R. H. Identification of genes differentially regulated by interferon alpha, beta, or gamma using oligonucleotide arrays. *Proc Natl Acad Sci U S A.* **95**, 15623–15628 (1998).
24. Hemmi, H. *et al.* Small anti-viral compounds activate immune cells via the TLR7 MyD88-dependent signaling pathway. *Nat Immunol.* **3**, 196–200 (2002).
25. Kawai, T. & Akira, S. Toll-like receptor and RIG-I-like receptor signaling. *Ann N Y Acad Sci.* **1143**, 1–20 (2008).
26. Yamamoto, M. *et al.* Role of adaptor TRIF in the MyD88-independent toll-like receptor signaling pathway. *Science.* **301**, 640–3 (2003).
27. Hoshino, K. *et al.* Cutting edge: Toll-like receptor 4 (TLR4)-deficient mice are hyporesponsive to lipopolysaccharide: evidence for TLR4 as the Lps gene product. *J Immunol.* **162**, 3749–52 (1999).
28. Hemmi, H. *et al.* A Toll-like receptor recognizes bacterial DNA. *Nature.* **408**, 740–5 (2000).
29. Mosca, J. D. & Pitha, P. M. Transcriptional and posttranscriptional regulation of exogenous human beta interferon gene in simian cells defective in interferon synthesis. *Mol Cell Biol.* **6**, 2279–83 (1986).

30. Diaz, M. O. *et al.* Homozygous deletion of the alpha- and beta 1-interferon genes in human leukemia and derived cell lines. *Proc Natl Acad Sci U S A.* **85**, 5259–63 (1988).
31. Chen, H. M. *et al.* Critical role for constitutive type I interferon signaling in the prevention of cellular transformation. *Cancer Sci.* **100**, 449–56 (2009).
32. Lutfalla, G. *et al.* Mutant U5A cells are complemented by an interferon-alpha beta receptor subunit generated by alternative processing of a new member of a cytokine receptor gene cluster. *EMBO J.* **14**, 5100–5108 (1995).
33. Velazquez, L. Fellous, M. Stark, G. R. & Pellegrini, S. A protein tyrosine kinase in the interferon alpha/beta signaling pathway. *Cell.* **70**, 313–22 (1992).
34. Lewerenz, M. Mogensen, K. E. & Uzé, G. Shared receptor components but distinct complexes for alpha and beta interferons. *J Mol Biol.* **282**, 585–99 (1998).
35. Shuai, K. *et al.* Interferon activation of the transcription factor Stat91 involves dimerization through SH2-phosphotyrosyl peptide interactions. *Cell.* **76**, 821–828 (1994).
36. Sarasin-Filipowicz, M. *et al.* Interferon signaling and treatment outcome in chronic hepatitis C. *Proc Natl Acad Sci U S A.* **105**, 7034–9 (2008).
37. Farnsworth, A. *et al.* Acetaminophen modulates the transcriptional response to recombinant interferon-beta. *PloS One.* **5**, e11031 (2010).
38. Mercer, D. F. *et al.* Hepatitis C virus replication in mice with chimeric human livers. *Nat Med.* **7**, 927–33 (2001).
39. Leung, S. *et al.* Role of STAT2 in the alpha interferon signaling pathway. *Mol Cell Biol.* **15**, 1312–1317 (1995).
40. Li, X. *et al.* Formation of STAT1-STAT2 heterodimers and their role in the activation of IRF-1 gene transcription by interferon-alpha. *J Biol Chem.* **271**, 5790–4 (1996).
41. Ghislain, J. J. & Fish, E. N. Application of genomic DNA affinity chromatography identifies multiple interferon-alpha-regulated Stat2 complexes. *J Biol Chem.* **271**, 12408–13 (1996).
42. Gupta, S. Jiang, M. & Pernis, A. B. IFN-alpha activates Stat6 and leads to the formation of Stat2:Stat6 complexes in B cells. *J Immunol.* **163**, 3834–41 (1999).
43. Perry, S. T., Buck, M. D., Lada, S. M., Schindler, C. & Shresta, S. STAT2 Mediates Innate Immunity to Dengue Virus in the Absence of STAT1 via the Type I Interferon Receptor. *PloS Pathogens.* **7**, e1001297 (2011).
44. Pattyn, E. *et al.* Dimerization of the interferon type I receptor IFNaR2-2 is sufficient for induction of interferon effector genes but not for full antiviral activity. *J Biol Chem.* **274**, 34838–45 (1999).
45. Platis, D. & Foster, G. R. Activity of hybrid type I interferons in cells lacking Tyk2: a common region of IFN-alpha 8 induces a response, but IFN-alpha2/8 hybrids can behave like IFN-beta. *J Interferon Cytokine Res.* **23**, 655–66 (2003).
46. McHutchison, J. G. *et al.* Telaprevir with peginterferon and ribavirin for chronic HCV genotype 1 infection. *N Engl J Med.* **360**, 1827–38 (2009).
47. Hézode, C. *et al.* Telaprevir and peginterferon with or without ribavirin for chronic HCV infection. *N Engl J Med.* **360**, 1839–50 (2009).
48. Kneteman, N. M. *et al.* HCV796: A selective nonstructural protein 5B polymerase inhibitor with potent anti-hepatitis C virus activity in vitro, in mice with chimeric human livers, and in humans infected with hepatitis C virus. *Hepatology.* **49**, 745–52 (2009).
49. Gutterman, J. U. Cytokine therapeutics: lessons from interferon alpha. *Proc Natl Acad Sci U S A.* **91**, 1198–1205 (1994).
50. Takeuchi, T. *et al.* Real-time detection system for quantification of hepatitis C virus genome. *Gastroenterology.* **116**, 636–642 (1999).
51. Yabuta, N. *et al.* Method for screening ligand having biological activity. PCT Int. Appl. WO0206838 (2002).
52. Inoue, K. *et al.* Evaluation of a cyclophilin inhibitor in hepatitis C virus-infected chimeric mice in vivo. *Hepatology.* **45**, 921–8 (2007).

Acknowledgments

This study was supported financially by Chugai Pharmaceutical Co., Ltd. H.K., K.O., Y.O., H.Y., H.O., M.A., A.O., H.S., N.H., A.K., K.M., T.T., N.S., Y.A., M.A. and M.S. are employees of Chugai Pharmaceutical Co., Ltd. We are grateful to George Stark for providing us the 2fTGH, U1A and U5A cell lines, and Akinori Takaoka for mouse Ifnar1-knockout MEFs. We also thank Isamu Kusanagi and Chiaki Tanaka for technical assistance, AVSS Co., Ltd. for technical assistance on EMCV, and Editing Services at Chugai Pharmaceutical Co., Ltd. for editorial assistance.

Author contribution statement

H.K., K.O., Y.O., H.Y., Y.H., A.O. and N.H. performed the experiments; H.K., K.O., H.O. and M.A. analyzed the data; G.F. and W.A. provided experimental materials and input into the data analysis; H.S., A.K., M.K., T.T., N.S., G.F., Y.A., M.A. and M.S. provided expert information; and H.K. and M.S. wrote the manuscript.

Additional information

Supplementary information accompanies this paper at http://www.nature.com/scientificreports

Competing financial interests: The authors declare no competing financial interests.

How to cite this article: Konishi, H. *et al.* An orally available, small-molecule interferon inhibits viral replication. *Sci. Rep.* **2**, 259; DOI:10.1038/srep00259 (2012).

FEBS Letters 586 (2012) 2318–2325

ELSEVIER

FEBS Letters

journal homepage: www.FEBSLetters.org

HSC90 is required for nascent hepatitis C virus core protein stability in yeast cells

Naoko Kubota [a,1], Yasutaka Inayoshi [a,1], Naoko Satoh [a,b], Takashi Fukuda [c], Kenta Iwai [a,b], Hiroshi Tomoda [c], Michinori Kohara [d], Kazuhiro Kataoka [e], Akira Shimamoto [e], Yasuhiro Furuichi [e], Akio Nomoto [f], Akira Naganuma [a], Shusuke Kuge [a,b,*]

[a] Laboratory of Molecular and Biochemical Toxicology, Graduate School of Pharmaceutical Sciences, Tohoku University, Aoba-ku, Sendai 980-8578, Japan
[b] Department of Microbiology, Tohoku Pharmaceutical University, Aoba-ku, Sendai 981-8558, Japan
[c] Department of Microbial Chemistry, School of Pharmaceutical Sciences, Kitasato University, Minato-ku, Tokyo 108-8641, Japan
[d] Department of Microbiology and Cell Biology, Tokyo Metropolitan Institute of Medical Science, Setagaya-ku, Tokyo 156-8506, Japan
[e] Gene Care Research Institute Co., Ltd., Kamakura, Kanagawa 247-0063, Japan
[f] Institute of Microbial Chemistry, Shinagawa-ku, Tokyo 141-0021, Japan

ARTICLE INFO

Article history:
Received 7 April 2012
Accepted 11 May 2012
Available online 31 May 2012

Edited by Hans-Dieter Klenk

Keywords:
Hepatitis C virus (HCV) core protein
Yeast growth defect caused by core protein
HSP90 inhibitor
Stability nascent polypeptide
HSC90
High-throughput screening

ABSTRACT

Hepatitis C virus core protein (Core) contributes to HCV pathogenicity. Here, we demonstrate that Core impairs growth in budding yeast. We identify HSP90 inhibitors as compounds that reduce intracellular Core protein level and restore yeast growth. Our results suggest that HSC90 (Hsc82) may function in the protection of the nascent Core polypeptide against degradation in yeast and the C-terminal region of Core corresponding to the organelle-interaction domain was responsible for Hsc82-dependent stability. The yeast system may be utilized to select compounds that can direct the C-terminal region to reduce the stability of Core protein.

1. Introduction

Chronic hepatitis C virus (HCV) infection causes liver cirrhosis and hepatocellular carcinoma [1]. Approximately 170 million individuals have been infected by HCV and are at risk for viral hepatitis, cirrhosis, and hepatocellular carcinoma [2]. HCV has a positive-strand RNA genome that encodes a polyprotein of ~3000 amino acids. The polyprotein is cleaved to yield the structural core, E1 and E2 polypeptides and seven non-structural polypeptides [3]. HCV core protein exhibits RNA-binding activity and is the major component of the viral nucleocapsid [4]. During HCV polypeptide synthesis, the core protein (Core, found at the N-terminus) is cleaved by a signal peptidase, releasing a protein 191 amino acids in length (Fig. 1A). The C-terminus of Core is further cleaved by a signal peptide peptidase at the endoplasmic reticulum (ER) membrane [5], which is required for virus production [6]. Generation of the mature Core (aa 1–177, $Core^{177}$) enables it to translocate to lipid droplets [7], where virion assembly is thought to occur. In addition to the direct role of the Core in viral production, expression of the Core induces lipid accumulation in hepatocytes and may be responsible for HCV-associated steatosis [8]. The Core has been implicated in the modulation of cellular processes that include lipid droplet reorganization, apoptosis, transformation, and host cell gene expression [9]. Thus, compounds that inhibit Core function or that reduce the stability of Core may also prevent the progression of HCV pathogenesis and viral production.

In this study, we established a system to screen compounds that reduce the stability of Core in the budding yeast *Saccharomyces cerevisiae*. We identified HSP90 (heat shock protein 90) inhibitors that reduce Core stability. Our results reveal that HSC90 (Hsc82) is required for the stability of the nascent Core in yeast cells. We found that the C-terminal domain of Core contributes to the stability of Core in yeast cells. The yeast system presented herein, which can be applied to high-throughput screening, may be useful for identifying for compounds that can direct a C-terminal domain to reduce the stability of the Core.

* Corresponding author. Address: Department of Microbiology, Tohoku Pharmaceutical University, 4-4-1 Komatsushima, Aoba-ku, Sendai, Miyagi 981-8558, Japan. Fax: +81 22 727 0129.
E-mail address: skuge@tohoku-pharm.ac.jp (S. Kuge).
[1] These authors equally contributed to this study.

0014-5793/$36.00
http://dx.doi.org/10.1016/j.febslet.2012.05.023

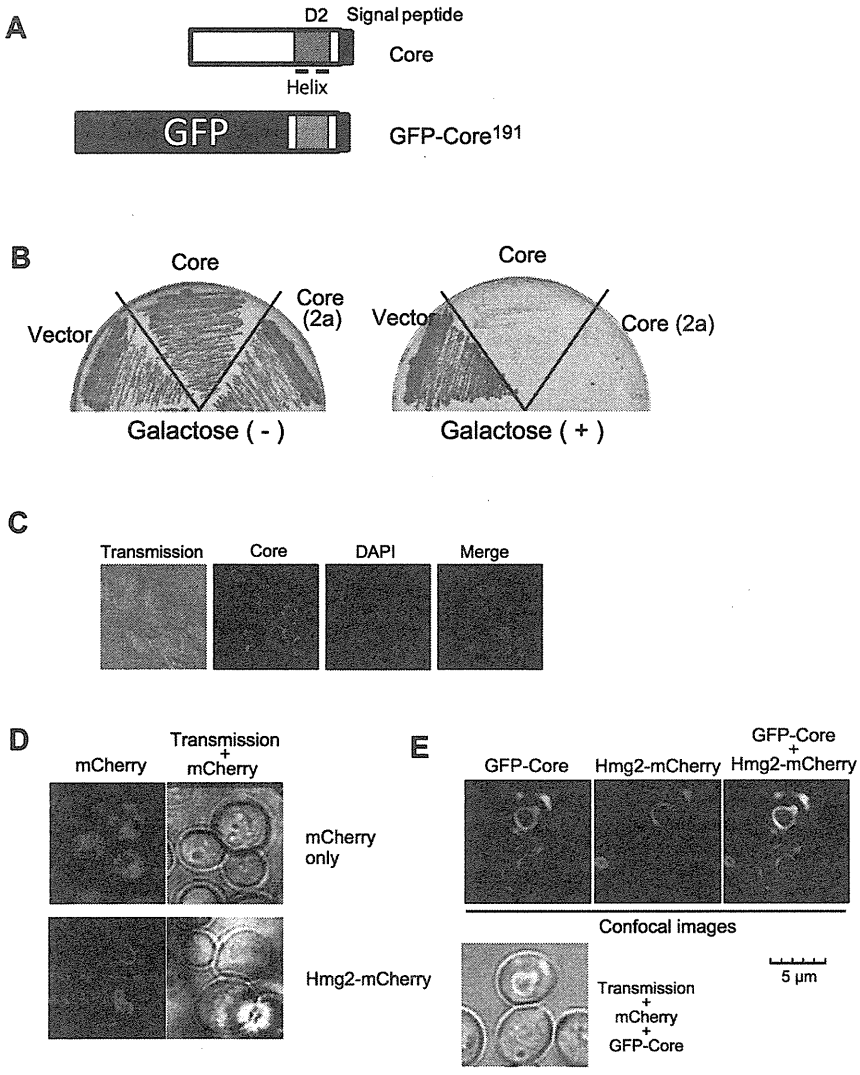

Fig. 1. HCV core protein-induced growth inhibition of yeast cells. (A) Schematic diagram of Core and GFP-Core[191]. Core protein contains a D2 domain (aa 118–171, shadowed boxes) including two helix structure and a Core-E1 signal peptide (aa 178–191, closed box). (B) Yeast cells carrying pRS425 (Vector), pRS425-GAL1-core (1b, aa 1–191) (Core) and pRS425-GAL1-core (2a, aa 1–191) (Core (2a)) were cultured on SR agar plates with (galactose +) and without (galactose −) 3% galactose for 60 h at 30 °C. (C) Core was induced in yeast cells carrying pRS425-GAL1-core for 2 h, fixed and examined using immunofluorescence assays. Nuclear staining was performed using DAPI (4′,6-diamidino-2-phenylindole, 2HCl). (D) The ER marker Hmg2-mCherry was localized to the perinuclear region. Confocal images of mCherry and Hmg2-mCherry fluorescence in wild-type yeast cells were monitored (ex. 543 nm; em. BA560IF). The confocal images were overlaid on a corresponding transmission image. (E) The GFP-fused Core D2 domain (GFP-Core, green) co-localized with Hmg2-mCherry (red). Confocal images of GFP were monitored (ex. 488 nm; em. BA505–525). Co-localization of GFP and mCherry and the transmission overlay are shown.

2. Materials and methods

2.1. Yeast strains, media, reagents and yeast transformation

Yeast cells were grown in a synthetic raffinose (SR dropout) medium [1.67% Bacto™ yeast nitrogen base lacking aminoacids (Difco) with 2% raffinose] supplemented with 0.04 mg/ml adenine and amino acids [SR dropout; [10]] at 30 °C. *S. cerevisiae* strains used in this study are indicated in the Supplemental Information.

2.2. Construction of plasmids for expression of HCV Core in yeast

To induce expression of the Core in yeast, we utilized a multicopy plasmid containing the *GAL1* promoter and the GAPDH terminator region (pKT10-GAL1) and a pRS425 [11] derivative containing the same *GAL1* promoter-GAPDH terminator region (pRS425-GAL1). The Core of HCV (1b) (hepatitis C virus isolate HCR6; GenBank accession no. AY045702) and pJFH1 (hepatitis C virus isolate JFH1; GenBank accession no. AB047639) were used. There are 11 amino acid differences within the D2 and the signal peptide between JFH1 and HCR6.

2.3. Screening for anti-Core chemicals

We examined the effects of various compounds isolated from microorganisms and known antibiotics (a library constructed in-house at the Kitasato Institute) as described in the Supplemental Information.